Spring 5-2018

Diastereoselective Synthesis of 2,4,6-Trisubstituted Piperidines via aza-Prins Cyclization

John A. Hood
University of Southern Mississippi

The University of Southern Mississippi

Diastereoselective Synthesis of 2,4,6-Trisubstituted Piperidines via aza-Prins Cyclization

by

John A. Hood

A Thesis
Submitted to the Honors College of
The University of Southern Mississippi
in Partial Fulfillment
of the Requirements for the Degree of
Bachelor of Science
in the Department of Chemistry and Biochemistry

May 2018

Approved by:

_____

Matthew G. Donahue, Ph.D., Thesis Advisor
Department of Chemistry and Biochemistry

_____

Vijay Rangachari, Ph.D., Chair
Department of Chemistry and Biochemistry

_____

Ellen Weinauer, Ph.D., Dean
Honors College

Abstract

The nitrogen heterocycles are shared amongst 59% of Food and Drug Administration (FDA) approved small molecule pharmaceuticals with the six-membered piperidine representing the most common moiety. Given the versatility and potential to yield derivatives with broad biological activities, the discovery of new chemical methods to generate these heterocycles in a more time and cost-efficient manner is desired. While there are existing racemic methods to access this class of molecule, the objective of this research is to pioneer a new novel six-step method to generate 2,4,6-trisubstituted piperidines with stereoselective control.

The first step is a condensation between a nonenolizable aldehyde and (*R*)-2-methylpropane-2-sulfinamide to create the Ellman *N*-sulfinyl imine. Carbons C3-C5 of the nascent ring can be installed at the *si* face of the imine via stereoselective allylation that is coordinated by transition metals such as magnesium, indium, or zinc to generate a homoallylic amine. The sulfinyl group is then removed via acidic conditions to afford the primary amine that is subsequently acylated with succinic anhydride to access an *N*-succinimide via a thermal condensation. A reduction of the cyclic imide via DIBAL-H accesses the *N*-acyl aminal. The ring closure is initiated by acidic activation of the enamine to the *N*-sulfinyl iminium ion. This positions the substrate into a kinetically favorable six-membered chair conformation that places the nucleophilic alkene to intercept the iminium carbon stereoselectively affording the tri-substituted piperidine. We are investigating this strategy as a tunable method to prepare a variety of stereochemically diverse piperidines.

Keywords: piperidine, heterocycles, organic synthesis, diastereoselective, medicinal chemistry, *N*-acyliminium ion

Dedication

For my loving mother, Dayni.

My best friend and who always has my back: even when I don’t have my own.

Acknowledgements

I would like to thank everyone who mentored and contributed to this work in some way. Above all, however, I would like to thank my thesis advisor Dr. Matthew G. Donahue for his unparalleled support these past years. I was extremely fortunate to have had the opportunity to work under such a supportive and driven mentor. Even through failures, Dr. Donahue's guidance was steadfast and instrumental in my successes, and without his patient, ambitious, and enthusiastic leadership, this work would have been insurmountable. I am proud to have been his student and cannot thank him enough for providing the single most transformative experience I had while at the University of Southern Mississippi.

I also want to extend a heartfelt thanks to Dr. Julie A. Pigza, my co-advisor, for welcoming me to her lab so early in my undergraduate career. That opportunity was the pivotal experience that inspired me to passionately pursue research. Even after departing her lab after sophomore year, she always made herself available to any questions or concerns I had while completing my thesis.

I would also like to thank all the past and present members of the Donahue and Pigza Research groups. I want to especially thank Nick Jentsch and Alison Hart for their coaching and advice as they always lent a helping hand. I wish them both success in their endeavors and hope that they bring their patient instruction wherever they go.

Lastly, I would like to thank the University of Southern Mississippi, the Honors College, and the Department of Chemistry and Biochemistry. Without their hospitality, support, and facilities, I would have not had such an amazing undergraduate experience.

Table of Contents

List of Figures

List of Schemes

List of Abbreviations

cm^{-1}	wavenumbers
^{1}H NMR	proton nuclear magnetic resonance
^{13}C NMR	carbon nuclear magnetic resonance
^{19}F NMR	fluorine nuclear magnetic resonance
Ac	acetyl
ATR	attenuated total reflectance
$B(OiPr)_3$	triisopropyl borate
$BF_3 \bullet OEt_2$	boron trifluoride diethyl etherate
˚C	celsius
$CDCl_3$	deuterated chloroform
CH_2Cl_2 or DCM	dichloromethane
CH_3CN	acetonitrile
COSY	correlated spectroscopy
d	doublet
D_2O	deuterium oxide
DEPT	distortionless enhancement by polarization transfer
DIBAL-H	diisobutylaluminium hydride
DMAP	4-dimethylaminopyridine
DMF	dimethylformamide
DMSO	dimethyl sulfoxide
equiv.	equivalent
Et	ethyl
Et_3N	triethylamine
FDA	Food and Drug Administration
FTIR	Fourier-transform infrared spectroscopy
g	grams

HCl	hydrogen chloride
HMBC	heteronuclear multiple bond correlation
HMDS	hexamethyldisilazane
HPLC	high performance liquid chromatography
HSQC	heteronuclear single quantum coherence
Hz	hertz
IR	infrared spectroscopy
J	coupling constant
LA	Lewis acid
M	molar
[M]	transition metal
Me	methyl
MeOH	methanol
$MgSO_4$	magnesium sulfate
MHz	mega Hertz
mg	milligram
mL	milliliter
mmol	millimole
NaOH	sodium hydroxide
nm	nanometer
NOESY	nuclear Overhauser effect spectroscopy
Nu	nucleophile
p-TSA	*para*-toluenesulfonic acid
Ph	phenyl
ppm	parts per million
q	quartet
Rf	retention factor
r.t.	room temperature

s	singlet
t	triplet
TFA	trifluoroacetic acid
THF	tetrahydrofuran
TLC	thin layer chromatography
TMS	trimethylsilane
Ts	tosyl
µL	microliter
µmol	mircomolar
UV/VIS	ultraviolet-visible spectroscopy
$ZnCl_2$	zinc chloride
δ	chemical shift

1. Introduction

Nitrogen heterocycles account for 59% of all FDA approved small molecules, with the six-membered piperidine scaffold representing the largest subpopulation of those nitrogenous ring systems.[1] The synthesis of piperidines is an active field of research given this heterocycle is an important building block for several therapeutic indications, such as antihistamines and analgesics.[2] While there are known procedures to produce multi-substituted piperidines, the objective of this research is to employ a new enantio- and diastereoselective six-step method to generate 2,4,6-trisubstituted piperidines.[3,4,5] The synthesis of enantiopure molecules is particularly relevant because nature creates large biomolecules, such as enzymes, with specific chirality that ultimately produce small molecules of specific handedness. In the body, pharmaceuticals often have increased benefit in the therapeutic indication if they complement nature's chiral complexes, thereby deeming a need for research to discover advanced synthetic methodologies to access molecules of one chirality.[6]

The synthesis of small molecules is an inescapable endeavor as many of today's products have roots in small molecules. Molecules that contain heterocycles are of significant interest today given their importance in a wide variety of economically important industries including agriculture, petroleum, and pharmaceuticals.[7] In particular, the non-aromatic piperidine heterocycle has emerged as a privileged scaffold in the pharmaceutical industry as shown in Figure 1.1. The piperidine bears one nitrogen and often occupies small molecule pharmaceuticals as a centralized scaffold to which different substituents can be arranged around. There is remarkable diversity in the structure and

substitution pattern of the piperidine scaffold in pharmaceuticals classifying it as a privileged moiety in small molecule drugs.[1]

Figure 1.1 Piperidine and Pharmaceutical Relevance

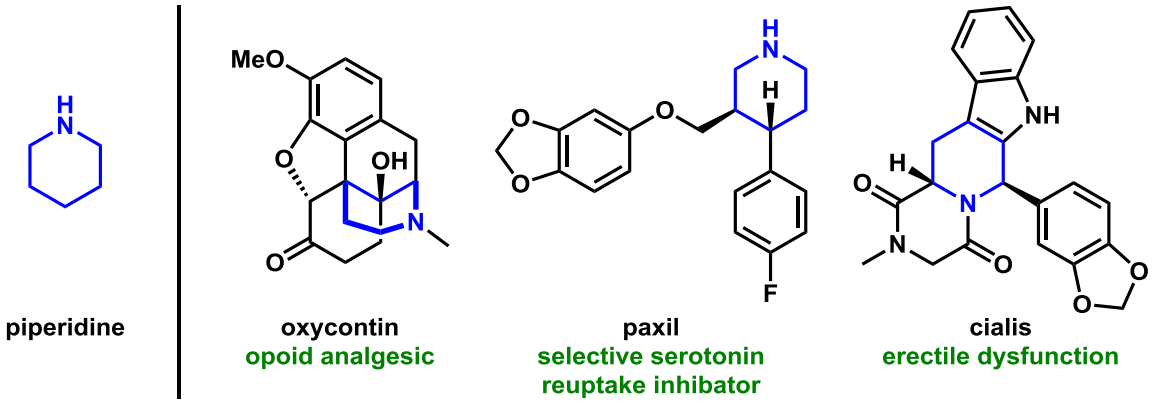

New estimates suggest that the research and development costs of bringing a new drug to market is well over 2.5 billion dollars.[7] On average, three years and 1.3 billion of those dollars are attributed to the production and screening of new small molecules, which poses a need for cost effective, time efficient methods to access new pharmaceuticals.[7] New methodologies in synthesis that expedite the production of molecules benefits all healthcare stakeholders as new pharmaceuticals can be more readily accessed and developed more economically.

The rate of new pharmaceutical drugs entering the market has slowed over recent years because of soaring production costs and more stringent federal regulations.[6] It takes over ten years of research and development to bring a new pharmaceutical to market.[7] This overwhelming obstacle is made worse by a low 11.8% success rate during clinical trials meaning many experimental drugs fail after several years in development.[7] The billions of dollars spent on unsuccessful molecules must be recovered through the marketing of other successful drugs that make it to market. The research presented here aims to combat high

costs and minimize production times of drug discovery by illuminating a new, robust synthesis route to generate the common piperidine moiety with enantioselectivity.

2. Literature Review

The generation of 2,4,6-trisubstituted piperidines poses a synthetic challenge as there are three non-contiguous chiral centers that must be set via transfer of chirality in a logical sequence. Chirality describes a geometric feature of molecules that are non-superimposable on their mirror image. This phenomena is observed with the carbon atom as it can have four unique substituents oriented in two ways generating *R*, right handed, and *S*, left handed, enantiomers as shown in Figure 2.1. Enantiomers have the same connectivity but differ in their spatial arrangement, meaning each molecule rotates plane-polarized light in a specific direction. Much like one's hands, there is a distinct left and right hand imposed by the arrangement of fingers. Chiral carbons exhibit this handedness and ensuring the correct chirality has been synthesized is critical for the access of natural products and drug synthesis. Complicating this issue are molecules that have more than one chirality center as multiple stereoisomers are possible. This introduces diastereomers, which are molecules with multiple configurations that differ in their stereocenters, but not at all positions, as this would describe enantiotopic behavior.

Chirality is a significant chemical property to pharmaceuticals because the body synthesizes proteins and enzymes with specific chirality, meaning chemists are challenged to emulate nature's processes to generating molecules of complementary chirality. This often enhances the therapeutic indication and grants access to the enantiopure molecules, which often improves the drug's success in clinical trials.

Figure 2.1 Importance of Chirality and Thalidomide Crisis

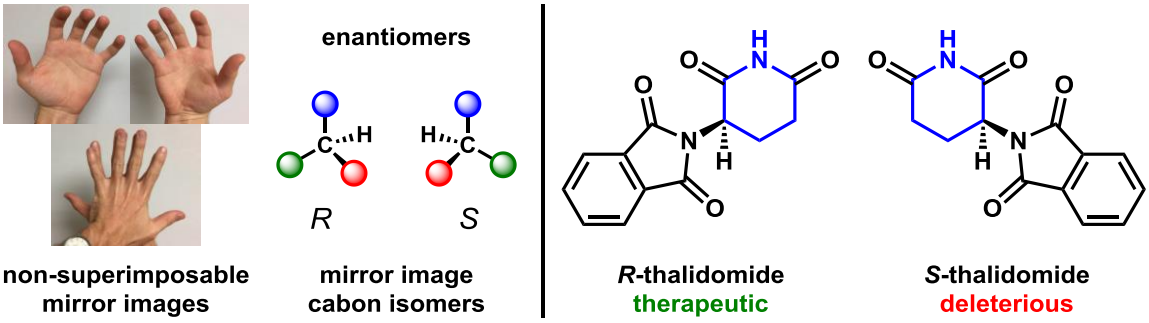

A specific example of the importance of chirality took place in the 1960s when thalidomide was prescribed to pregnant mothers to attenuate morning sickness. While *R*-thalidomide was therapeutic, the *S*-thalidomide was determined to be a teratogen that had deleterious effects on fetal development and resulted in many limb deformities called phocomelia as shown in Figure 2.1.[7] Following that crisis, the FDA has since mandated drugs be more rigorously characterized and studied before entering the market to minimize the risk of detrimental drugs reaching the public.[7] This means that racemic – mixtures of *R* and *S* enantiomers – and diastereotopic pharmaceuticals take longer to evaluate because each stereoisomer must be thoroughly examined as each exhibits unique chemical behaviors *in vivo*. While this decision benefits public health, the synthesis of drugs has been made more challenging, and demands the discovery of stereoselective reaction procedures to generate enantiopure molecules.

Although there are established strategies to produce substituted piperidines, the reported methodologies have limitations in accessing enantiopure trisubstituted piperidines in high yield. The synthetic approaches often utilize *N*-acyliminium ions in which an intramolecular cyclization is initiated under acidic conditions with an alkene nucleophile as shown in Figure 2.2.

Figure 2.2 Lewis Acid Cyclization Strategies

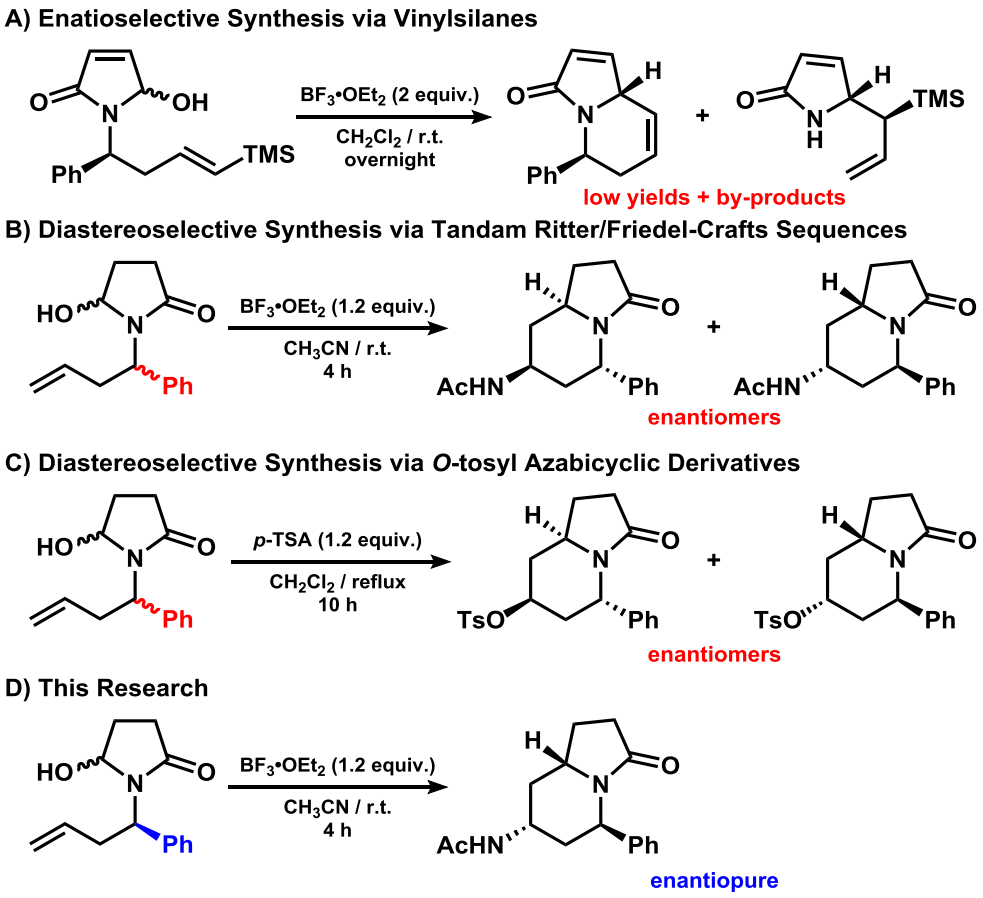

Reported in 2009, the synthesis of an enantiopure disubstituted piperidine was established using a *N*-acyl aminal and vinylsilane nucleophile under Lewis acid conditions as shown in **(A)** in Figure 2.2.[9] While this methodology was stereoselective, the yields were dismal at 25% as the vinylsilane often produced undesired allylsilanes and other byproducts. This methodology was improved later through the use of a intramolecular cyclization coupled with nitrile and arene trapping agents in which Ritter or Friedel-Crafts sequences were employed as shown in Figure 2.2 **(B)**.[3] This generated trisubstituted piperidines with high diastereoselective control and good yields, and similarly, another group exercised a *para*-toluenesulfonic acid route with similar success as shown in Figure 2.2 **(C)**.[10] Although these methods are successful in accessing desired chirality, these

synthetic routes generated racemic mixtures of products. This limitation is a result of the racemic starting materials, and therefore, this research would benefit from the identification of methodologies to readily synthesize enantiopure starting materials. The objective of this research is to discover a methodology to yield enantiopure starting materials for the aforementioned diastereoselective conditions to generate enantiopure trisubstituted piperidines.

3. Methodology

3.1 Retrosynthesis

Scheme 3.1 Retrosynthetic Analysis of 2,4,6-Trisubstituted Piperidines

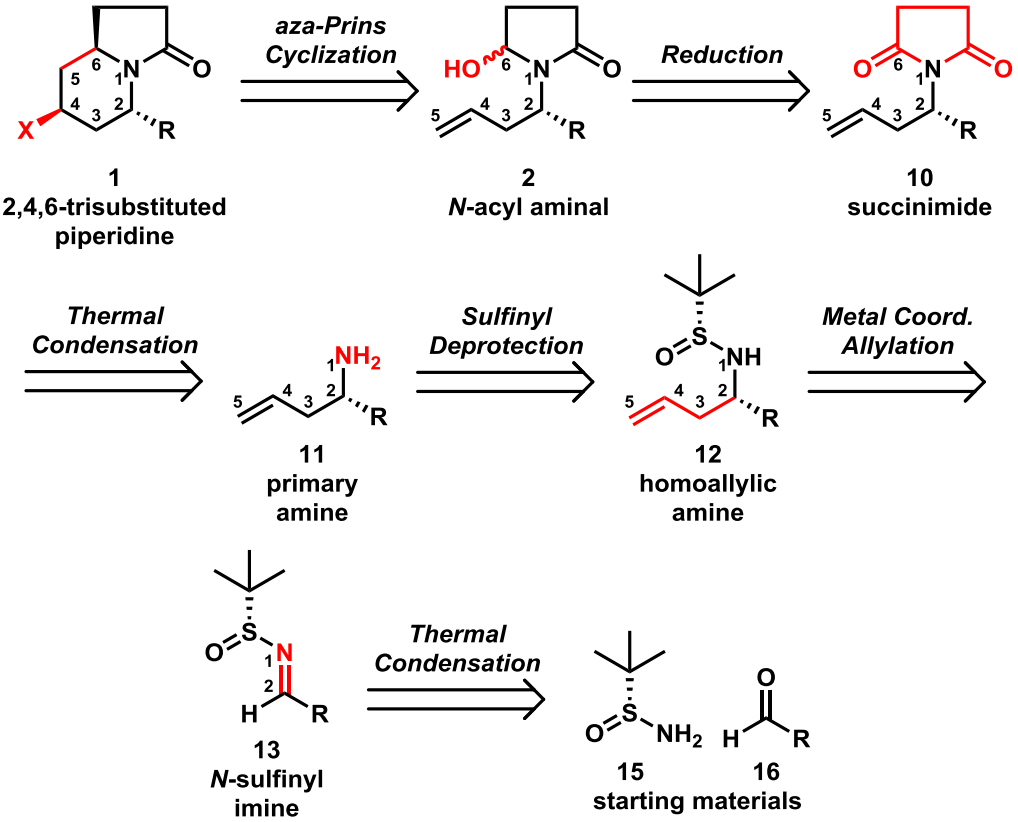

To pioneer a new synthetic route to access 2,4,6-trisubstituted piperidines with stereoselective control, a retrosynthetic approach was used to plan the synthesis of the

desired product from readily available, low-cost starting materials as shown in Scheme 3.1. It was hypothesized that the presented six-step synthetic route could be employed to access structurally diverse enantiopure 2,4,6-trisubstituted piperidines in a new way.

Analyzing the trisubstituted piperidine **(1)**, the bond between C-6 and C-5 was cleaved to open the heterocycle. Use of the *N*-acyl aminal **(2)** synthon, shown in Scheme 3.2, provided the ideal precursor given its previous use and that it provides all required carbons and reactive species for an intramolecular cyclization.

Scheme 3.2 Mechanistic Proposal of aza-Prins Cyclization

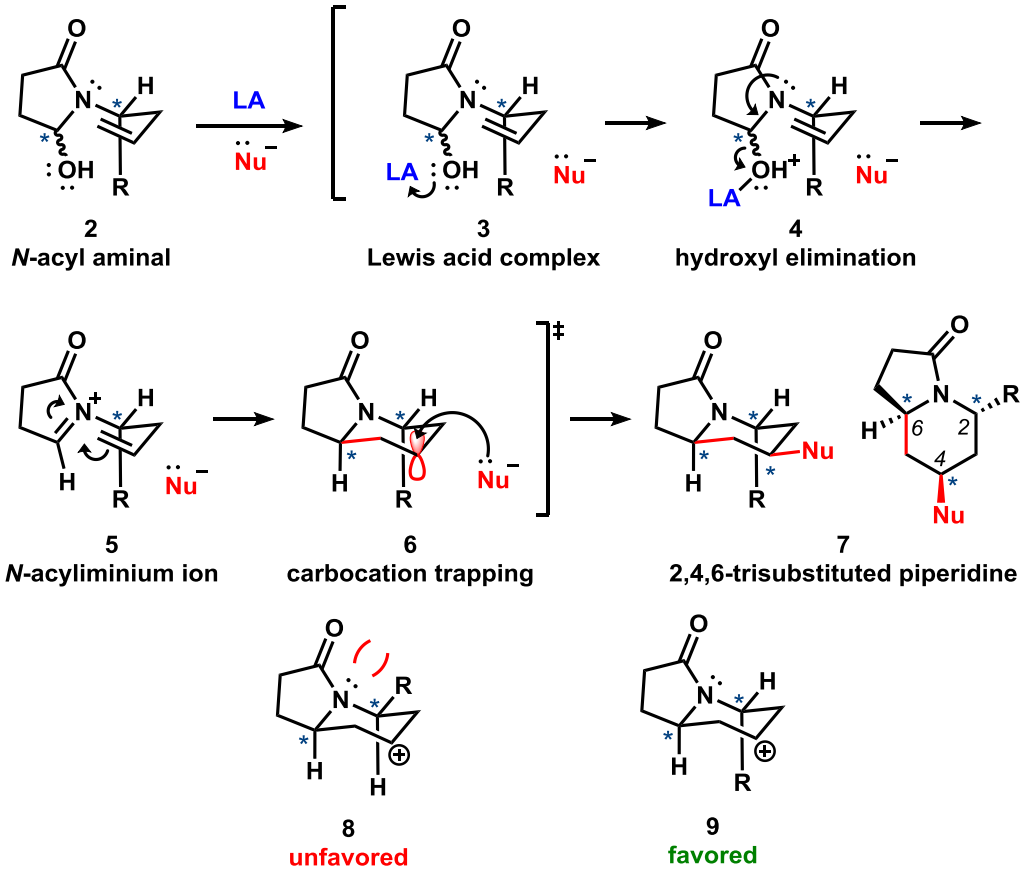

Placing a hydroxyl group on the carbon directly adjacent to the nitrogen allows for a Lewis acid to coordinate with the *N*-acyl aminal to form a Lewis acid complex **(3)** to enhance the hydroxyl for elimination. The nitrogen at N-1 can then donate its electrons to

the bond between the flanking carbon to cleave the hydroxyl group **(4)**. The placement of a terminal alkene at C-5 provides the intramolecular nucleophile and is hypothesized to intercept the *N*-acyliminium ion **(5)** with stereoselective control during the cyclization because of strong allylic strain and steric hindrance.[3] The more thermodynamically favorable chair-like transition state places the R substituent in the axial position **(9)** during intermolecular cyclization because the substrate exhibits lower (1,3) allylic strain between the alkene and R and less steric hindrance between the oxygen and R. R in the equatorial position is unfavored **(8)** because of greater allylic strain and steric hindrance meaning the energy barrier is higher and favors the R in the axial position. The nascent carbocation **(6)** will then be trapped at the equatorial position to generate the trisubstituted piperidine **(7)**.

The generation of the *N*-acyl aminal **(2)** synthon will be afforded from a reduction of one of the carbonyls in succinimide **(10)** using sodium borohydride as shown in Scheme 3.1. Although this reduction should generate a diastereotopic mixture of substrates, the proposed formation of the *N*-acyliminium ion eliminates the hydroxyl group prior to the ring closure and yields an enantiopure substrate for the cyclization. The succinimide **(10)** synthon will be accessed via a double condensation reaction with succinic anhydride and the primary amine **(11)**. The primary amine nitrogen serves as the nucleophile and attacks the succinic anhydride twice with an acid intermediate.[11] This sets the last carbon required for the forming piperidine, C-6, while simultaneously placing the carbonyl needed for the reduction step.

The homoallylic amine **(12)** synthon will be synthesized by a sulfinyl deprotection in which the chiral sulfinyl group will be cleaved from the molecule using acidic and basic conditions. Then, a metal coordinated allylation reaction with allyl bromide will install C-

3, C-4, and C-5 of the desired piperidine and the terminal alkene nucleophile required for the cyclization. The allylation must be stereoselective as the chirality at this carbon will be relayed to the other stereocenters during the cyclization. Literature denotes a variety of metals have coordinated with *N*-sulfinyl imines **(13)** to organize a diastereoselective attack via a bicyclic chairlike transition state **(14)** that positions the metal in coordination with the oxygen and nitrogen of the sulfinyl group as shown is Scheme 3.3.[12] The metal simultaneously supports the chair-like transition state directing the bulky tertbutyl group down and activates the imine to nucleophilic attack. The positioning of the tertbutyl group down blocks the *re* imine face, meaning that the allyl bromide nucleophile can intercept only the top, *si* face of the imine. This step sets the first carbon stereocenter at C-2 of the forming piperidine and generates the enantiopure homoallylic amine **(12)**.

Scheme 3.3 Transition Metal Coordinated Allylation of *N*-Sulfinyl Imines[12]

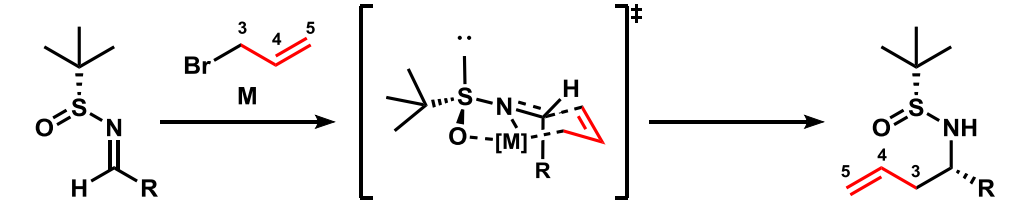

13
***N*-sulfinyl imine**

14
transition state

12
homoallylic amine

The *N*-sulfinyl imine **(13)** synthon will be accessed via a thermal condensation reaction between (*R*)-2-methyl-2-propanesulfinamide **(15)** and a nonenolizable aldehyde **(16)**. These reagents in the presence of a Lewis acid solvent and moderate heat should generate imines with great yields. This reaction serves to provide the carbon and substituent at position C-2 of the forming piperidine and installs the chiral auxiliary, 2-methyl-2-propanesulfinamide, required for the stereoselective allylation. Fortunately, the 2-methyl-2-propanesulfinamide is commercially available in either *R* and *S* enantiomers meaning

both can be readily employed to synthesize either enantiomer of the trisubstituted piperidine proposed by this route. Additionally, there are numerous structurally diverse nonenolizable aldehydes commercially available at low cost, meaning a broad substrate scope can be explored and structurally diverse trisubstituted piperidines may be accessed via this methodology if successful.

3.2 General Laboratory Techniques

While the reactions are proceeding, thin layer chromatography (TLC), high performance liquid chromatography (HPLC), and proton nuclear magnetic resonance (^{1}H NMR) were employed to monitor the reaction progress. TLC is chromatography technique commonly employed to monitor reaction progress as it is cost effective, highly sensitive, and time efficient. It works by spotting the base line of a silica gel plate with a desired sample. The plate is then placed in a solvent chamber where solvent travels up the plate to separate the components of a reaction solution based on polarity. The separated components can then be visualized under ultraviolet light or stained to visualize spots on the plate. Measuring the fraction of the distance traveled by the component in relation to the solvent front yields an Rf value in which spots can be quantitatively compared. Running reaction starting materials in parallel to ongoing reactions allowed for convenient reaction progress monitoring in which consumption of starting material spots and formation of new spots in the reaction's lane signified reaction completion.

HPLC is another chromatography technique in which components are separated based on polarity similar to TLC, but this technique offers more resolution and computer integration to quantitatively measure the reaction progress. The HPLC in the Donahue Research Group is an Agilent reverse phase system equipped with an UV/VIS detector for

detecting chromophores: light absorbing molecules. Samples are automatedly loaded and travel to a column that separates the components of a sample by polarity. Each component has a unique retention time and generated unique peaks that was used to quantitively compare components of a sample. Running the chromophore reactants before beginning the reaction allowed for the identification of new compounds as new peaks materializing during the reaction signified reaction progress. It is important to note that both TLC and HPLC are important techniques, but they could become convoluted and hard to interpret if many reagents, undesired byproducts, or reaction intermediates formed. This made reaction monitoring difficult at times as these methods only provided clues to what is occurring in the reaction vessel.

The last technique commonly used to monitor reaction progress was proton nuclear magnetic resonance (^{1}H NMR). The instrument works by placing the hydrogen nuclei of a sample into a magnetic field to measure their Larmor frequency. Each unique hydrogen nuclei in a compound exhibits a predictable precession in a magnetic field and generates calculable peak(s) on a computerized spectrum. These peaks were then used to elucidate the structure of compounds present in a sample. In reaction monitoring, the peaks of the starting materials were followed for their disappearance while new product peaks materialized.

Once the reaction was complete and the desired product was isolated, an extensive spectral analysis was initiated to verify the formation of the desired products. Proton nuclear magnetic resonance (^{1}H NMR) and carbon nuclear magnetic resonance (^{13}C NMR) are one dimensional NMR techniques used to identify the unique hydrogen and carbon nuclei in the sample. This technique generates a two-dimensional plot with peaks resulting

from nuclei Larmor frequencies. Following those experiments, two distortionless enhancement by polarization transfer (DEPT) carbon experiments were then run to determine the multiplicity of the carbon nuclei. The DEPT135 spectrum orients the CH and CH_3 peaks up while the CH_2 peaks point down. This allows for easy determination of CH_2 peaks, but CH and CH_3 require a second experiment. The DEPT90 spectrum isolates the CH peaks and exclusively presents them in the up orientation, which allowed for quick identification of CH_3 carbon signals by process of elimination.

Two-dimensional NMR techniques such as homonuclear correlation spectroscopy (COSY), heteronuclear single quantum correlation (HSQC), and heteronuclear multiple bond correlation (HMBC) were also employed. A COSY spectrum places the ^{1}H NMR spectrum on both the vertical and horizontal axes with an internal plot of proton cross-peaks. This plot is useful as neighboring protons will produce correlations between protons three and four-bond distances away, which allowed for elucidation of specific spin systems within the molecules. HSQC is similar to COSY except the vertical axis is replaced with the ^{13}C NMR, and the cross-peaks generated on the internal plot represented correlations between protons and their directly attached aliphatic carbons. This allowed for convenient assignment of protons to respective carbons. HMBC's spectrum is similar to HSQC in that the horizontal axis bears the ^{1}H NMR and the vertical axis bears the ^{13}C NMR, but the cross-peaks generated by this spectrum are correlations between carbons and protons separated by two, three, and four-bond distances away. This allows for chains of atoms to be elucidated from one proton signal. By identifying chains and their overlapping partners, the connectivity of the generated molecules could be elucidated to identify chemical structures.

The last 2D NMR technique to be employed was nuclear Overhauser effect spectroscopy (NOESY). A NOESY spectrum places a ^{1}H NMR spectrum on both the vertical and horizontal axes similar to COSY, but instead of through bond correlations resulting, cross-peaks of through-space correlations are observed when nuclei are close to each other.

Following the NMR suite of experiments, a drop of the NMR sample was loaded onto a Fourier-transform infrared spectrometer (FTIR) equipped with an attenuated total reflectance (ATR) attachment to measure the absorption of electromagnetic radiation. This instrument fires infrared radiation into a sample inducing atoms and groups of atoms within organic compounds to vibrate. Each covalent bond in a compound will absorb and vibrate predictably at a specific frequency that can then be quantized and displayed in a two-dimensional spectrum to determine potential functional groups. While NMR detects unique nuclei, FTIR reveals specific groups of atoms which is valuable in identifying fragments of the generated molecules and aided in identification of chemical structures.

High resolution mass spectrometry (HRMS) determined the sample's exact mass to four decimal points which was useful to differentiating molecular formulas that have the same nominal mass. Optical rotation determines the extent to which a molecule rotates plane-polarized light. This phenomenon is a characteristic of chiral molecules as they are optically active and provided a data set to characterize chirality. The most comprehensive analysis to identifying molecular structure though is X-ray crystallography in which X-rays of the molecule are obtained to generate an electron density map. This image can then be processed to reveal the absolute positions of all atoms which grants the ability to determine the absolute configuration of the chemical structure.

4. Results

4.1 Ellman Condensation of Aldehydes to form *N*-Sulfinyl Imines

To initiate the synthetic route, (*R*)-2-methyl-2-propanesulfinamide **(17)** and a broad scope of nonenolizable aldehydes **(18)** were chosen. A nonenolizable aldehyde is one in which there are no alpha hydrogens that could potentially form the imine tautomer called an enamine. A variety of aldehydes were selected containing common synthetic functional groups of differing inductive effects to investigate this route's versatility to chemically unique substrates.

Scheme 4.1 Ellman Condensation

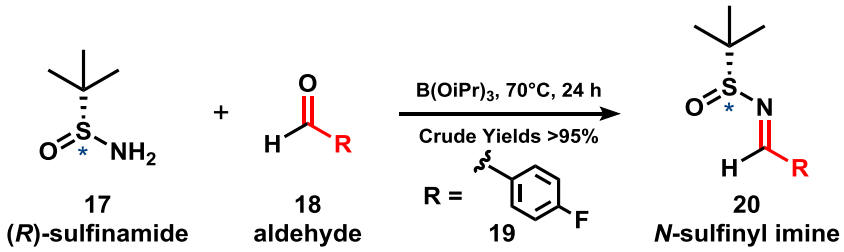

The *para*-fluorobenzaldehyde **(19)** will generally serve as the substrate described throughout this synthesis as it was the first substrate committed to this synthetic route. The fluorine of the *para*-fluorobenzaldehyde is ^{19}F NMR active which aided in the elucidation of reaction progress and identification of generated molecules. All substrates chosen are shown in Figure 4.1 and range in electron withdrawing and donating activity.

The first step is a condensation reaction in which one equivalent of aldehyde **(18)** was reacted with 1.2–1.25 equivalents sulfinamide **(17)** at 80˚C in triisopropyl borate solvent. Triisopropyl borate is not only the solvent but a Lewis acid that activates the aldehyde for attack by the weakly nucleophilic amine group. The excess sulfinamide is employed to

ensure that all aldehyde is converted to the desired *N*-sulfinyl imine by Le Chatelier's principle.

Figure 4.1 *N*-Sulfinyl Imines Synthesized

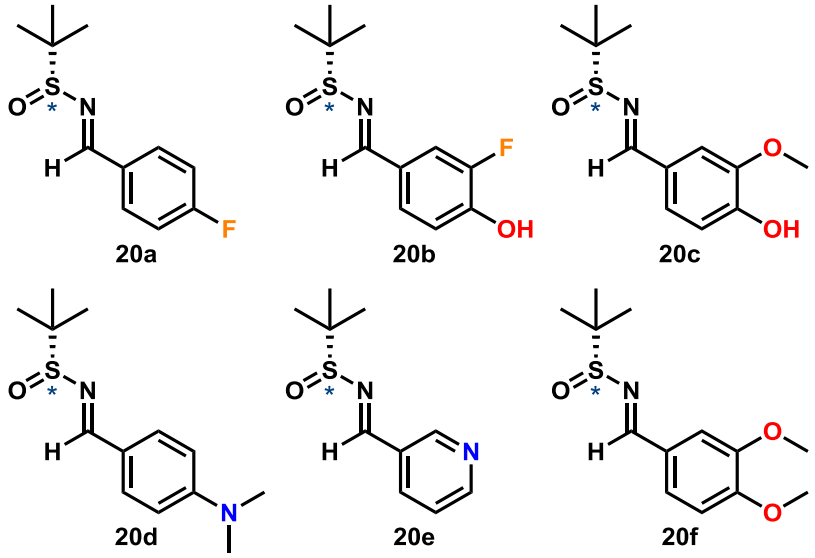

All condensation reactions were completed within 48 hours as monitored via HPLC by comparing starting material retention times with new peak retention times. In every instance, the starting aldehydes had shorter retention times than the desired *N*-sulfinyl imines. The HPLC data for the reaction of *para*-fluorophenyl *N*-sulfinyl imine **(20a)** is shown in Figure 4.2. The top spectrum was recorded at the reaction start with *para*-fluorobenzaldehyde giving a retention time of 4.2 minutes. After 22 hours, the bottom spectrum shows the *para*-fluorobenzaldehyde peak was consumed, and a new peak at 6.4 minutes had materialized signifying the end of the reaction.

Figure 4.2 Reaction Monitoring of Ellman Condensation Reactions via HPLC at 254 nm

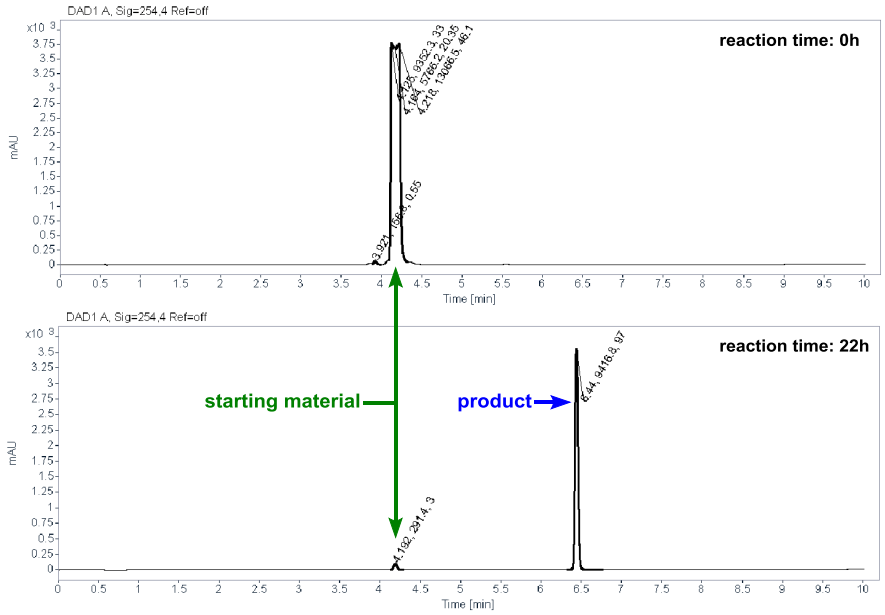

Upon completion, the reactions were cooled to room temperature, diluted with water and ethyl acetate, and stirred vigorously for one hour. The organic layer was then extracted once, dried with magnesium sulfate, and gravity filtered before concentration via rotary evaporator. The identification of desired product was carried out using ^{1}H NMR since the characteristic imine peak was found at 8 ppm. Further, the absence of the aldehyde CH peak at 10 ppm confirmed the consumption of the starting aldehyde. For example, the *para*-fluorophenyl *N*-sulfinyl imine ^{1}H NMR is shown in Figure 4.3.

All *N*-sulfinyl imines featured this general spectral characteristic that aided in the quick identification of the desired products at this step. Fortunately, these reactions proceeded smoothly with all substrates producing high yields (>95%). The crude product was immediately subjected to the next step without purification. All substrates following workup had a minor impurity probably resulting from the use of the triisopropyl borate as ^{1}H NMRs of crude products had some small peaks in the 1.5 ppm region. This reaction was favorable as there were no complicated preparation of glassware or anhydrous conditions

required. Further, these reactions may be left to age for several hours after completion without worry of any major hydrolysis by-products forming, making this a robust, straightforward strategy to afford many structurally diverse *N*-sulfinyl imines.

Figure 4.3 ^{1}H NMR of *para*-Fluorophenyl N-Sulfinyl Imine from Ellman Condensation

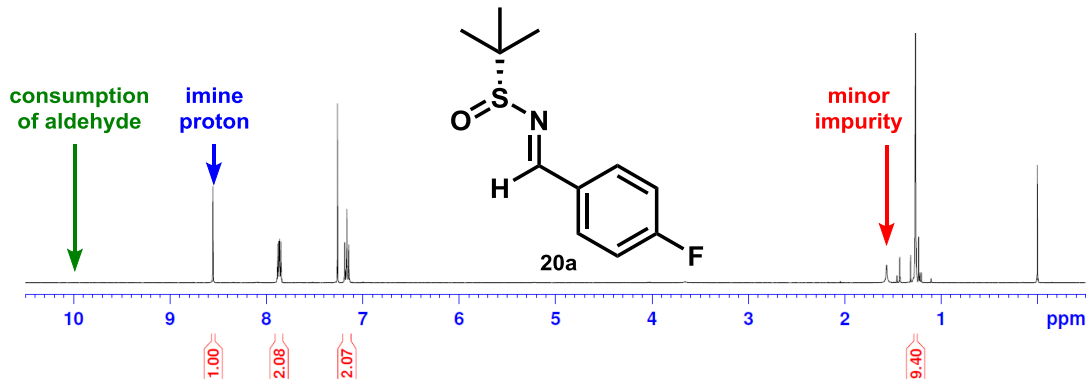

4.2 Metal Coordinated Allylation

Several publications have reported stereoselective allylations of *N*-sulfinyl imines in which transitions metals magnesium, zinc, and indium had been employed to generate homoallylic amines with high stereoselective control.[12,13,14,15,16] The use of magnesium to form the Grignard reagent was first employed in this research given its commonality in organic synthesis. However, this reaction was successful in generating the homoallylic amine in 61% yield, the production of diastereomers was observed in a ratio of 6:1 as determined by ^{1}H NMR with major and minor allyl peaks at 5.7 ppm as shown Figure 4.4. Given the subpar diastereoselection coupled with the high cost of the Grignard reagent and labor-intensive reaction vessel setup, other transition metals were investigated.

Figure 4.4 Diastereomers of *N*-Sulfinyl Imine from Grignard Reaction

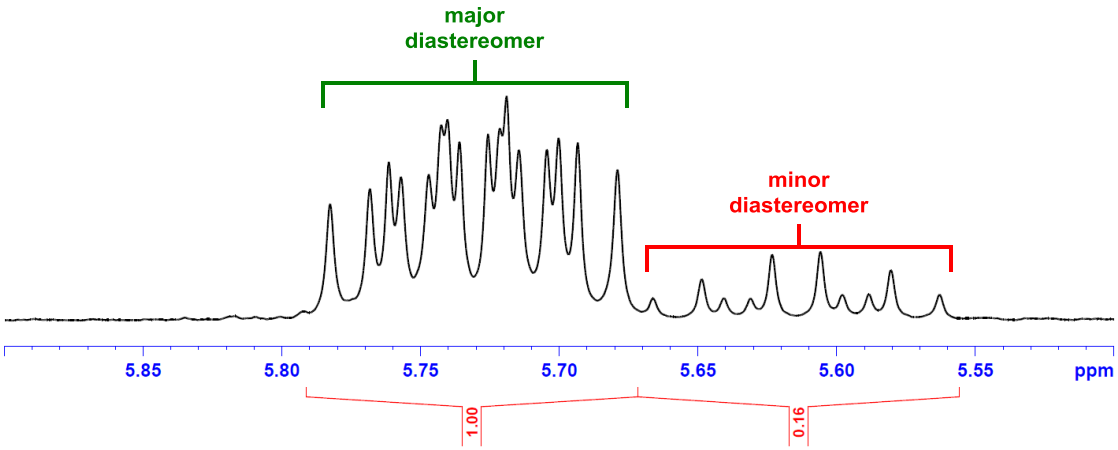

Zinc has been employed successfully in allylations with *N*-sulfinyl imines via aza-Barbier conditions.[14,15] The cost of zinc was considerably lower than the organomagnesium reagent and eliminated the need for anhydrous conditions, providing this as an exciting alternative. Zinc flakes were activated by washing in 1.0 N aqueous HCl to remove the oxidation layer on its surface. The activated zinc, *N*-sulfinyl imine, and allyl bromide were then reacted to net a mixture of diastereomers and unreacted imine starting material as shown in Figure 4.5. It was interesting to observe that the zinc metal favored the opposite diastereomer from the Grignard reaction in approximately 3:1 ratio.

Figure 4.5 Diastereomers of *N*-Sulfinyl Imines from Zinc Reaction

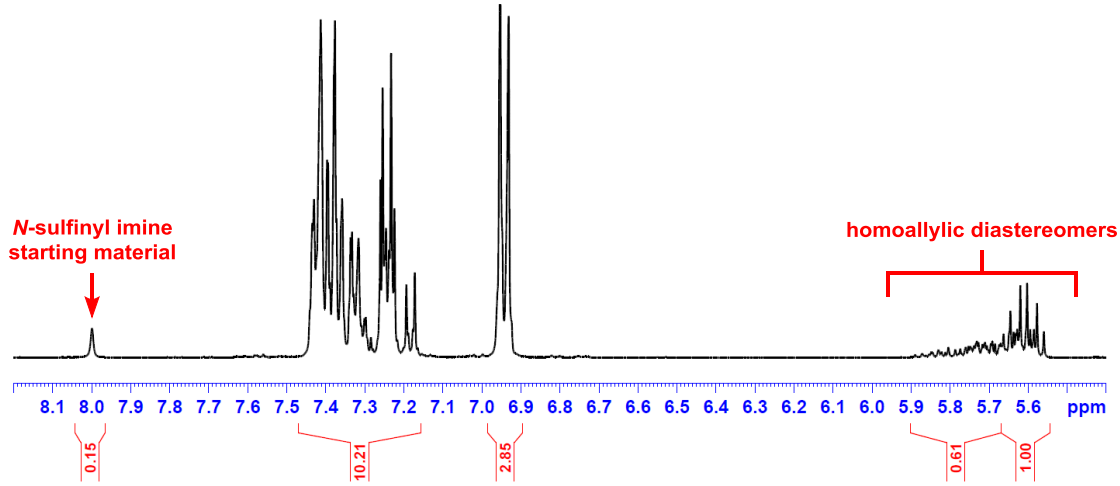

It was then hypothesized that increasing the surface area of the zinc by employing zinc powder would enhance the reaction's yields and stereoselectivity because the zinc would have more exposed surface area to coordinate the stereoselective attack. Unfortunately, similar low conversion rate and lackluster stereoselectivity was observed again: even when using several excess equivalents of activated zinc. A major shortcoming observed from the literature was the omission of procedures used for the activation of zinc. Given these disappointing results employing zinc and the arduous activation protocols, the use of zinc metal was abandoned altogether.

Scheme 4.2 Indium Coordinated Allylation

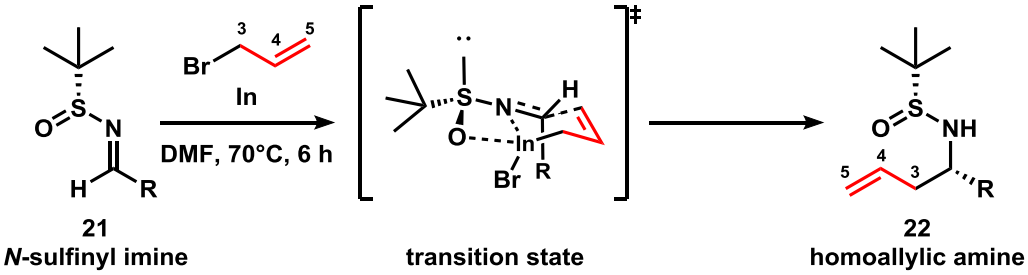

More recently, approaches include indium metal under similar conditions to the aforementioned zinc methodologies.[16] The indium approach generated the *para*-fluoro homoallylic amine **(22a)** in 82% yield. ^{1}H NMR of the *para*-fluoro homoallylic amine, Figure 4.6, revealed the consumption of starting material with a small *N*-sulfinyl imine residue peak at 8.6 ppm.

The stereoselectivity was far improved from preceding metal trials with only one set of allyl peaks observed at 5.7 ppm and means a diastereotopic ratio greater than 20:1 was achieved. The formation of diastereotopic peaks at 2.5 ppm further validates the formation of desired product with the only minor impurity carried from the previous condensation reaction. Indium was the most efficient allylating reagent as it could be used without

activation and was not water sensitive. These features eliminate costs of activation, increases ease and maximizes reproducibility, making indium the ideal candidate for the synthesis of homoallylic amines.

Figure 4.6 Enantiopure Allylation of *para*-Fluoro Homoallylic Amine ^{1}H NMR

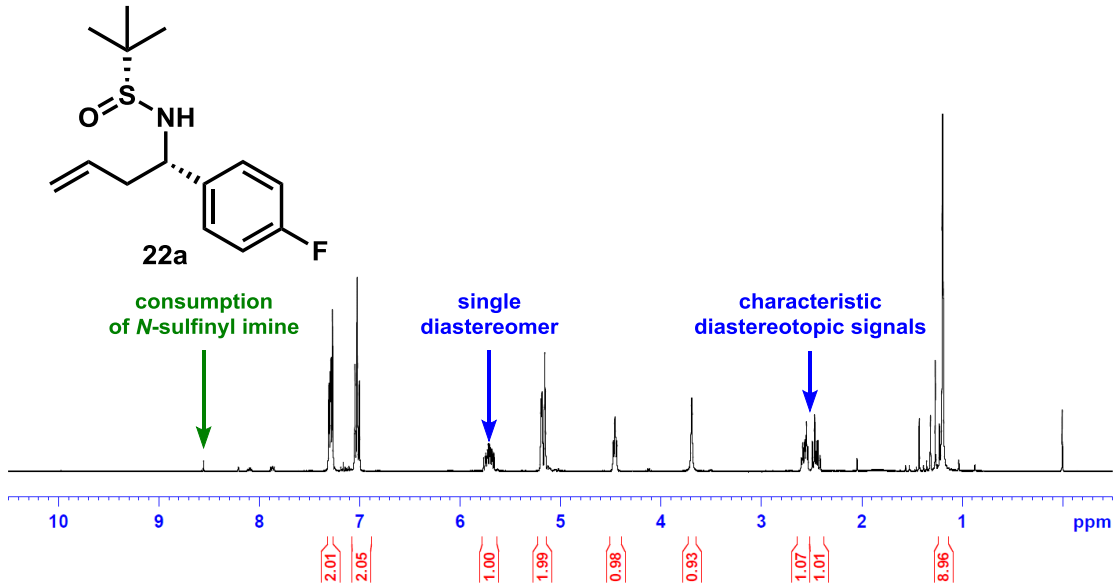

4.3 Deprotection of Homoallylic Amine to form Free Base

The deprotection of homoallylic amines **(22)** proceeded within minutes with high yield.[12,17] The homoallylic amines were dissolved in diethyl ether and immediately chilled to 0˚C. Three equivalents of 4M HCl in dioxane were then added, and within seconds, the reaction completed with a thick white precipitate forming in the flask. The white precipitate was found to be the desired ammonium salt **(23)** and offered a convenient step in which the ammonium salt solid was vacuum filtered using a Buchner funnel. This filtration purified the desired material from the eliminated *tert*-sulfinyl group and the residual impurities from the preceding steps. ^{1}H NMR of the white precipitate verified the removal of the sulfinyl group as the large *tert*-butyl peak at 1.2 ppm was no longer present, and the

formation of a new, broad peak at 8.6 ppm confirmed the synthesis of the desired ammonium salt. The sulfinyl deprotection generated a white precipitate for all substrates and provided yields greater than 80%.

Scheme 4.3 Sulfinyl Deprotection of Homoallylic Amines

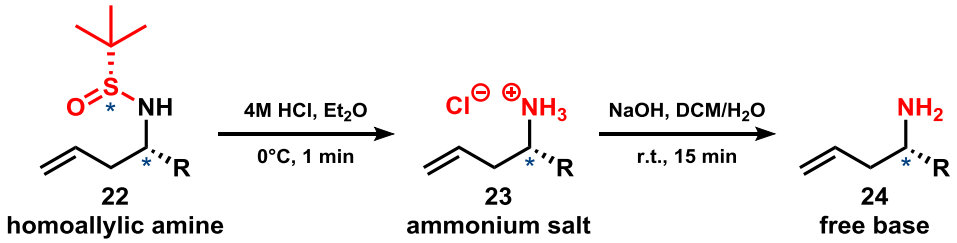

Since the sulfinyl deprotection proved reliable in many trials, the ammonium salts were immediately subjected to basic conditions to afford the free base **(24)**. To a solution of 10:1 dichloromethane (DCM)/water, ammonium salt was reacted with two equivalents of sodium hydroxide pellets. The reaction was allowed to stir for fifteen minutes before the free base was collected via extraction with dichloromethane. Careful attention was needed at this step as minimizing the amount of water utilized prevented the loss of desired product to the aqueous phase. ^{1}H NMR confirmed the generation of desired free base as a new broad peak at 1.7 ppm was found as shown in Figure 4.7.

Figure 4.7 Deprotected *para*-Fluorophenyl Homoallylic Amine ^{1}H NMR

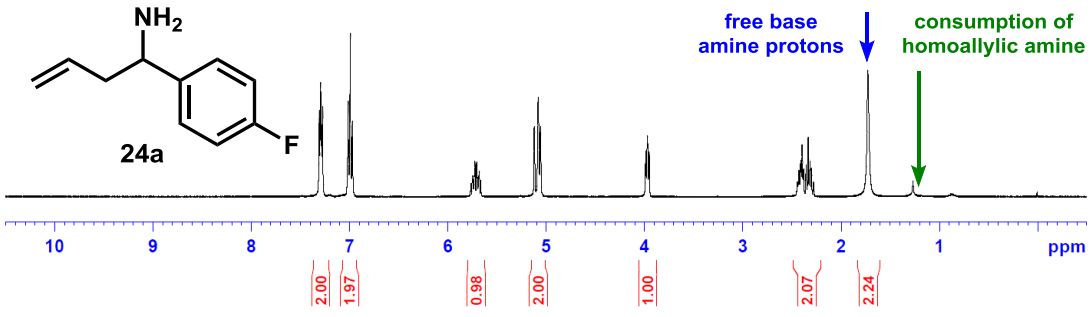

4.4 Condensation of Succinic Anhydride to form Succinimide

Several publications have detailed condensation reactions to access succinimides using a mild organic base at reflux in toluene.[18,19] Utilizing the published conditions, equal equivalents of free base **(24)** and succinic anhydride **(25)** were dissolved in toluene. Then two equivalents of triethylamine were added, and the reaction was allowed to age for two hours at 115˚C. TLC revealed the consumption of free base with the spot at Rf 0.35 being consumed, and a new spot at Rf 0.21 materialized. The reaction was then analyzed by ^{1}H NMR and revealed the intermediate acid amide **(26)** had formed with no desired succinimide **(27)**. A peak at 6.9 ppm was characteristic of the amide functional group along with additional peaks at 2.5 ppm resulting from the protons on the uncyclized product.

Scheme 4.4 Thermal Condensation to Generate Acid Amide

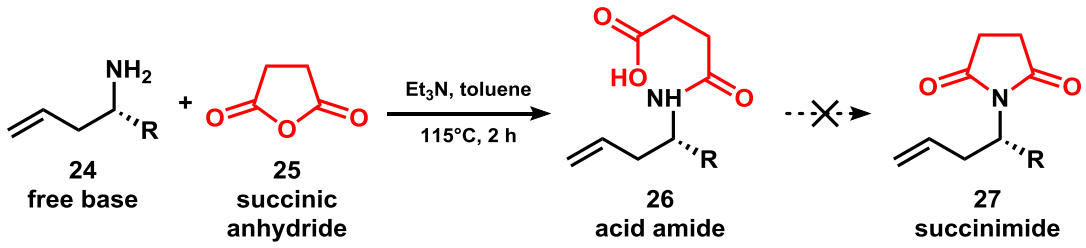

In an effort to drive the reaction to completion, the crude acid amide was then resubmitted to toluene and triethylamine and microwaved for thirty minutes. Unfortunately, the higher temps and electromagnetic radiation had no effect, and the acid amide persisted without any succinimide formation. It was hypothesized that the water generated by the first condensation reaction hindered the reactivity of the substrate and prevented the acid amide from cyclizing. Other works denoted use of a Dean Stark apparatus to collect and remove water from the reaction to access the succinimide, but

those methodologies generally took greater than 24 hours and generated succinimides in modest yields.[20]

Another method using zinc chloride ($ZnCl_2$) and hexamethyldisilazane (HMDS) offered succinimides in high yields within hours; given these time advantages over the previous procedures, this methodology was used.[21] Equal equivalents of free base and succinic anhydride were dissolved in toluene, and then 1.5 equivalents of HMDS and 1 equivalent of $ZnCl_2$ were added. The reaction was heated to 85˚C and monitored via TLC. After two hours, new spots formed indicating the desired products were forming as shown in Figure 4.8.

Figure 4.8 TLC Reaction Monitoring of Succinimide Formation

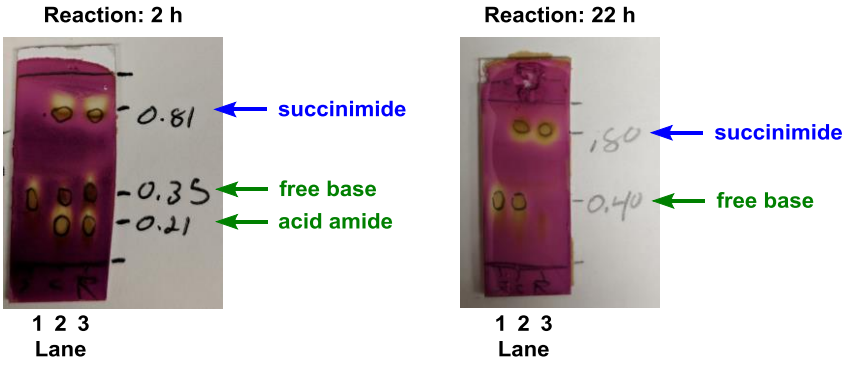

In lane one was the free base starting material with Rf 0.35. Lane three contained the reaction mixture in which some free base and acid amide was observed as spots at Rf 0.35 and Rf 0.21 after two hours. However, the new spot at Rf 0.81 hinted at the formation of the succinimide, and therefore the reaction was allowed to proceed for an additional 20 hours to allow for the complete consumption of free base and acid amide. After 22 hours, TLC revealed the consumption of both the free base and acid amide as only the spot at Rf 0.81 was observed. The reaction was then allowed to cool to room temperature and worked

up. ^{1}H NMR revealed a characteristic singlet at 2.6 ppm with integration of 4 indicating that the desired succinimide was generated as shown in Figure 4.9.

Figure 4.9 ^{1}H NMR of para-Fluoro Succinimide

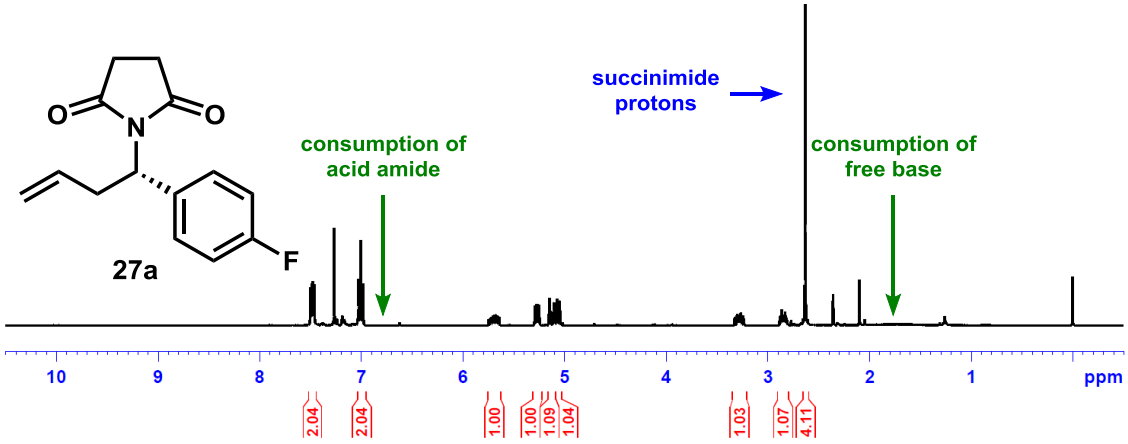

The complete consumption of the free base and acid amide was observed as no peaks from those substrates remained. Further, this reaction generated no major impurities and therefore the succinimide crude products obtained from this method were submitted to the next step without purification.

4.5 Reduction of Succinimide and Cyclization to Trisubstituted Piperidine

The reduction of the succinimide to the *N*-acyl aminal is well documented using sodium borohydride.[9,10,22] Succinimides **(27)** were dissolved in methanol, cooled to 0˚C, and 1 equivalent of $NaBH_4$ was added as shown in Scheme 4.5. Monitoring the reaction progress via TLC revealed the succinimide starting material persisted even after several hours without the formation of no new material. The reaction was then allowed warm to room temperature as it was hypothesized the additional heat would drive the advancement of the reaction. After allowing to stir for three hours at room temperature, the reaction was worked up, and ^{1}H NMR revealed the reaction failed to produce any *N*-acyl aminal **(28)**.

Scheme 4.5 Reduction of Succinimide with $NaBH_4$

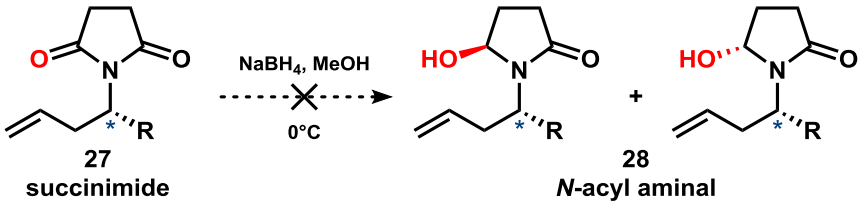

It was then theorized that the succinimide would require additional equivalents of $NaBH_4$ to access the *N*-acyl aminal and so the collected succinimide was resubmitted to the reduction conditions with an additional equivalent of $NaBH_4$. Reaction monitoring via TLC revealed that the succinimide spot continued to persist with no new material forming. An additional six equivalents of $NaBH_4$ were added in an effort to consume the succinimide, and the reaction was allowed to stir overnight. The next day, TLC revealed

Figure 4.10 ^{1}H NMR of Sodium Borohydride Reduction

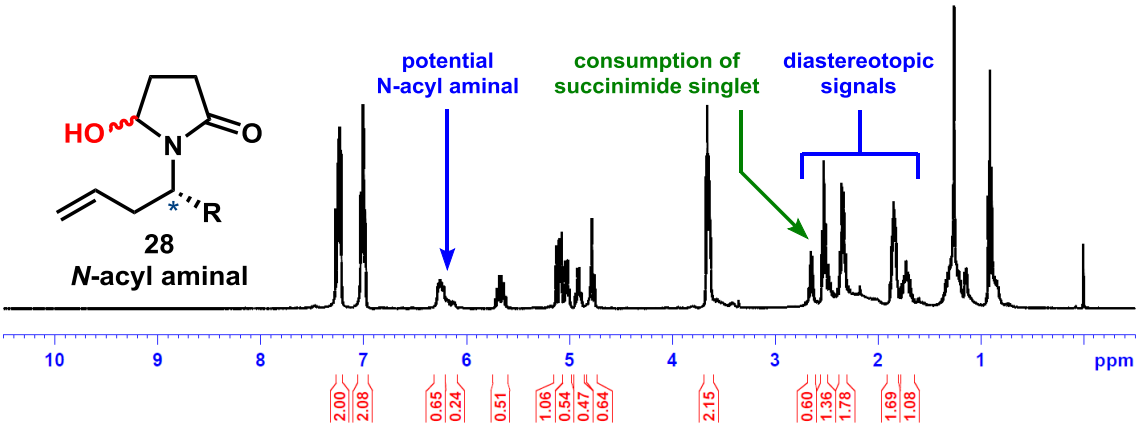

succinimide was consumed, and a new spot had materialized near the bottom of the TLC plate. This was inspiring as the *N*-acyl aminal was hypothesized to be more polar and materialize lower on the plate. The ^{1}H NMR showed several new peaks at 7.3, 6.2, and 2.5 ppm that were indicative of *N*-acyl aminal formation as shown in Figure 4.10.

It was anticipated that the reduction would not be stereoselective and the generation of diastereomers would be observed, meaning a remarkably complex ^{1}H NMR was

anticipated. Since a complicated spectrum was generated, it was assumed that the *N*-acyl aminal was accessed even though ^{1}H NMR was too convoluted to confirm. A purification was considered at this point to isolate the diastereomers; however, the separation would have posed very challenging as the *N*-acyl aminal is rather reactive. Purification conditions may have destroyed the *N*-acyl aminal, and so to validate if the *N*-acyl aminal was accessed, the crude reaction material was submitted to the cyclization conditions under the assumption it would convert to the trisubstituted piperidine.[3] Monitoring the reaction via ^{1}H NMR, peaks at 7.3, 6.2, and 2.5 ppm should have disappeared if the desired *N*-acyl aminal was generated; however, these peaks persisted, and no new product peaks were observed. Ultimately, it was determined that the reduction was unsuccessful, and that an undesired, unidentified over-reduced byproduct was obtained. This material was abandoned, and a new reduction agent was employed to access the *N*-acyl aminal.

Scheme 4.6 Reduction of Succinimide with DIBAL-H

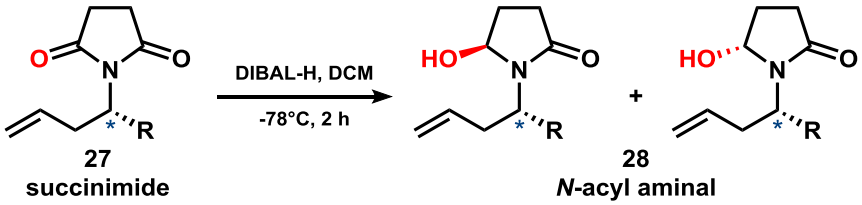

27
succinimide

28
***N*-acyl aminal**

DIBAL-H is a common stochiometric reducing reagent and was chosen given soluble nature in inert organic solvents such as DCM, hexanes, or toluene. The succinimide **(27)** was dissolved in an anhydrous solution of DCM, and then the vessel was cooled to -78˚C as shown in Scheme 4.6. Slowly, one equivalent of DIBAL-H was added dropwise with care not to warm the reaction. The cooled reaction was monitored via TLC for two hours revealing that reaction progress stalled 15 minutes after the addition of DIBAL-H as succinimide was still present. Additional equivalents of DIBAL-H were avoided as it was

assumed the formation of over reduced byproducts would occur. ^{1}H NMR showed new minor alkene peaks at 5.7 ppm buried under the alkene peak of the succinimide, and new diastereomer peaks found at 2.5 ppm indicated that the desired *N*-acyl aminal **(28)** had been produced as shown in Figure 4.11. It was then inferred that the succinimide would have no reactivity under the cyclization conditions meaning the best method to proceed was to submit the crude reaction material to the next step to access the trisubstituted piperidine. The reaction could then be purified without worry of eliminating the *N*-acyl aminal.

Figure 4.11 ^{1}H NMR of Successful Reduction with DIBAL-H

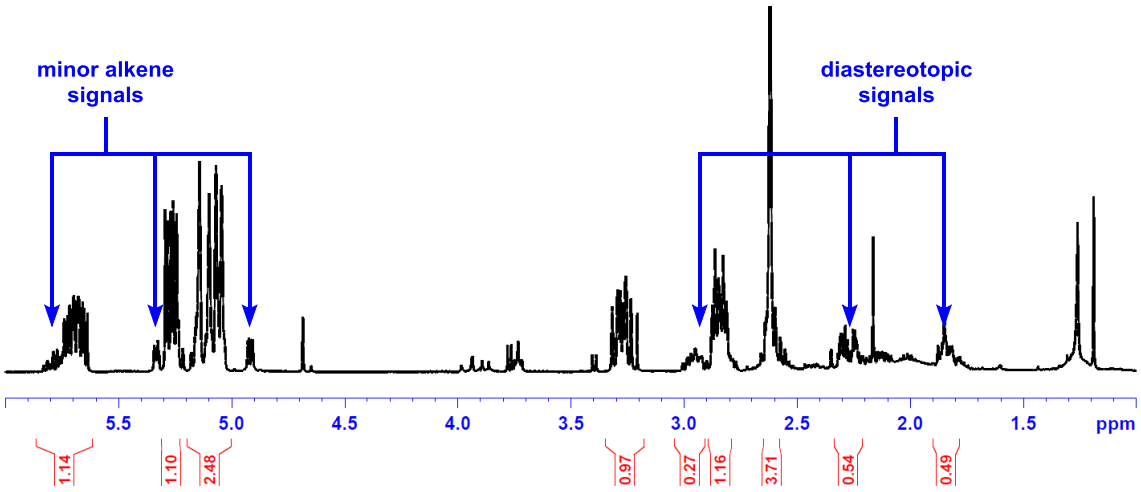

The crude reaction mixture was then submitted to the cyclization conditions by dissolving into deuterated acetonitrile and adding one equivalent of boron trifluoride diethyl etherate (BF_3•OEt_2). The reaction was monitored via ^{1}H NMR, and it revealed partial conversion of the proposed *N*-acyl aminal peaks as the intensity of the minor peaks in the alkene region, 5.7 ppm, were consumed and new peaks in the 4.0 ppm range materialized. These were indicative signals of a successful cyclization, although resolving the ^{1}H NMR with majority succinimde and *N*-acyl aminal remaining made absolute identification impossible. A purification was needed to remove the succinimide. The

purification proceeded smoothly using 5% methanol in DCM to afford 10 mg of white solid. ^{1}H NMR confirmed the desired trisubstituted piperidine **(29)** had been synthesized as the alkene peaks had been completely consumed, and the formation of characteristic peaks at 5.4, 4.0, and 2.6 ppm were observed as shown in Figure 4.12. Generation of the piperidine also validated that the reduction was successful in generating the *N*-acyl aminal as the cyclization would not have occurred without that substrate.

Figure 4.12 ^{1}H NMR of *para*-Fluoro 2,4,6-Trisubstitued Piperidine

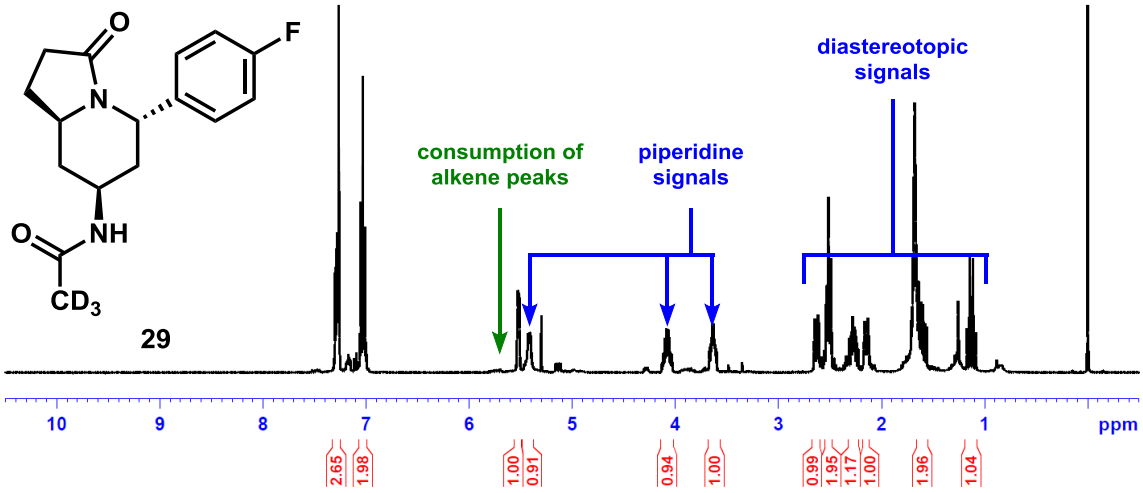

Examining the ^{1}H NMR closer, the peak at 5.4 ppm was determined to be the N-H amide proton, H_a, of the trisubstituted piperidine as shown in Figure 4.13. The number of peaks a proton signal can produce is calculated using Pascal's triangle and the equation $2^n = X$ in which "n" equals the number of unique neighboring nuclei and X equals the number of peaks. Since the amide proton has one neighbor proton, H_b, the equation results to $2^1 = 2$ meaning the signal is split into two peaks generating a doublet (d). Each split of a peak is the result of nuclei coupling and is measured in hertz between the signal's crests to quantify the intensity of interaction between the nuclei. The 7.1 Hz coupling observed here is characteristic of vicinal, three-bond distances, coupling between protons H_a and H_b.

Figure 4.13 Amide Proton Splitting Tree

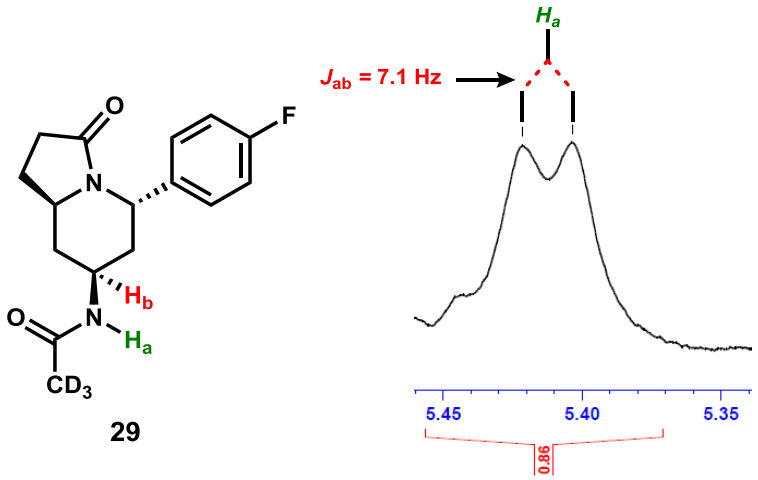

This proton peak was also much broader than other peaks in the spectra indicative of the distinctive N-H coupling as nitrogen's unique spin quantum number affects the quadrupole relaxation during the examination. HSQC validated this proton belonged to the amide as it was the only proton signal that had no correlation to any carbon nuclei within the molecule. Compiling this information, this was the most straightforward proton to identify as all others found in this molecule exhibited more complex splitting patterns.

One such example is the proton observed at 2.6 ppm in the ^{1}H NMR. As shown in Figure 4.14, the chair conformation **(30)** proton H_a has four coupling neighbors resulting in the equation $2^n = X$ to be $2^4 = 16$ theorizing the signal was to be split four times into 16 peaks. This was observed in the height intensities of the proton signal in which a ratio of 1:2:2:2:1:1:2:2:2:1 was generated. Each of the four neighbors had a unique coupling constant that split each other and ultimately formed a doublet of doublet of doublet of doublet (dddd) peak. H_b was two-bond distances away and resulted in the largest, 13.6 Hz germinal coupling. H_d and H_c were three-bond distances away and produced 3.5 Hz and 1.7 Hz vicinal couplings respectively. Their lower hertz value was a result of their greater distance and dihedral angle in relation to H_a. The Karplus equation defines the coupling of

protons with a 90˚ relationship to exhibit smaller coupling constants, while anti or eclipsed protons exhibit larger coupling constants.[23] The Newman projections in Figure 4.14 display the dihedral angle of H_c, **(A)** and H_d **(B)** in relation to H_a as close to 90˚ and serves to explain their small coupling constants.

Figure 4.14 Splitting Tree of 1H at 2.63 ppm

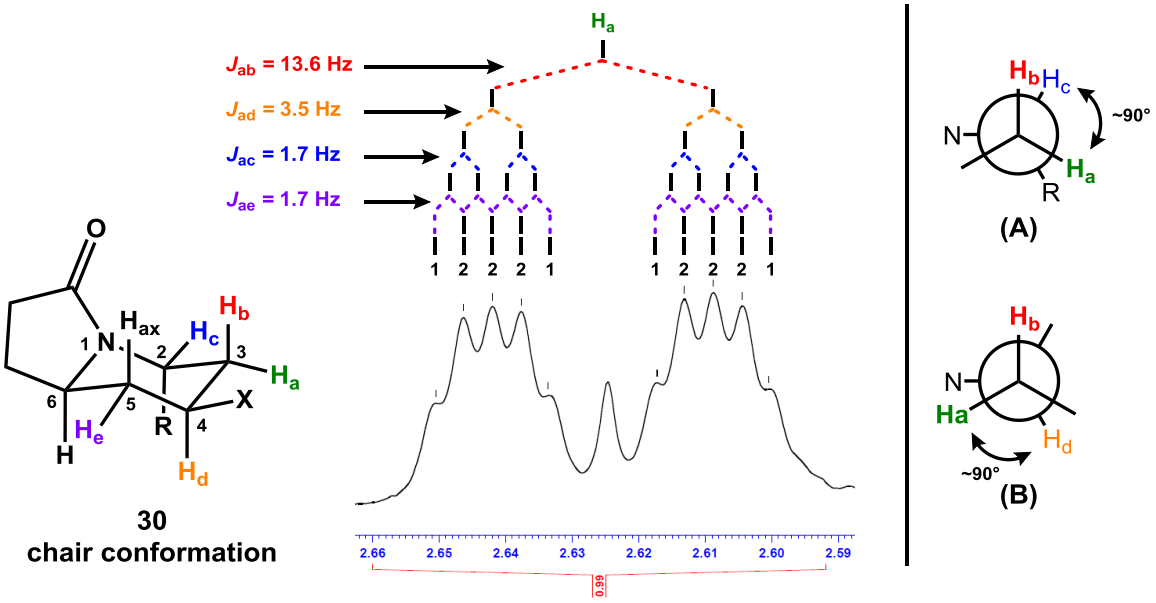

H_e was the farthest coupled proton in which W-coupling resulted. This coupling is four-bond distances away from H_a and resulted from the geometrically favorable chair conformation that six-membered heterocycles exhibit. The W-coupling gets its name from the w shape of the four bonds that make up the connectivity of the equatorial protons that exhibit this unique coupling. W coupling is characteristically between 1 and 3 hertz because of the far distance between nuclei. Axial protons do not exhibit W-coupling and explains why H_{ax} exhibited no coupling with H_a as the geometric relationship prevents coupling. Lastly, the H_e proton signal at 2.15 ppm confirms w coupling with H_a as its splitting tree contains a complimentary 1.7 Hz coupling constant meaning that both nuclei

are splitting each other. All these relationships serve as important observations in confirming the structure of the generated trisubstituted piperidine.

It is important to note that the ^{1}H NMR of the trisubstituted piperidine indicated no apparent minor diastereomer as no minor peaks were observed. This indicates that the cyclization was stereoselective and offers promise of a stereoselective procedure. To validate whether this methodology generated an enantiopure trisubstituted piperidine, crystals of the substrate will have to be grown and sent for X-ray crystallography. This means that a subsequent trial needs to be run on a larger scale in the future to obtain more material as only enough was employed in this initial experiment to suffice as proof of concept.

4.6 Cyclization via Alternative Michael Addition Pathway

An alternative four step method to access enantiopure trisubstituted piperidines was envisioned in which a vinylogous amide was hypothesized to form the *N*-iminium ion under acidic conditions and induce the cyclization via trapping of a carbocation as shown in Figure 4.15. This method diverges from the aforementioned strategy after step two in which the homoallylic amine **(31)** is subjected to a Michael addition reaction with ethyl propiolate **(32)** to place a double bond adjacent to the nitrogen. This was proposed to generate a vinylogous amide **(33)** that could subsequently be subjected to acidic conditions, such as trifluoroacetic acid **(34)**, to induce formation of the *N*-iminium ion **(35)** thus allowing the pendant alkene to attack via an aza-Prins cyclization. This forms the carbocation intermediate **(36)** to which a conjugate base can trap and yield the trisubstituted piperidine **(37)**.

Figure 4.15 Michael Addition and aza-Prins Cyclization

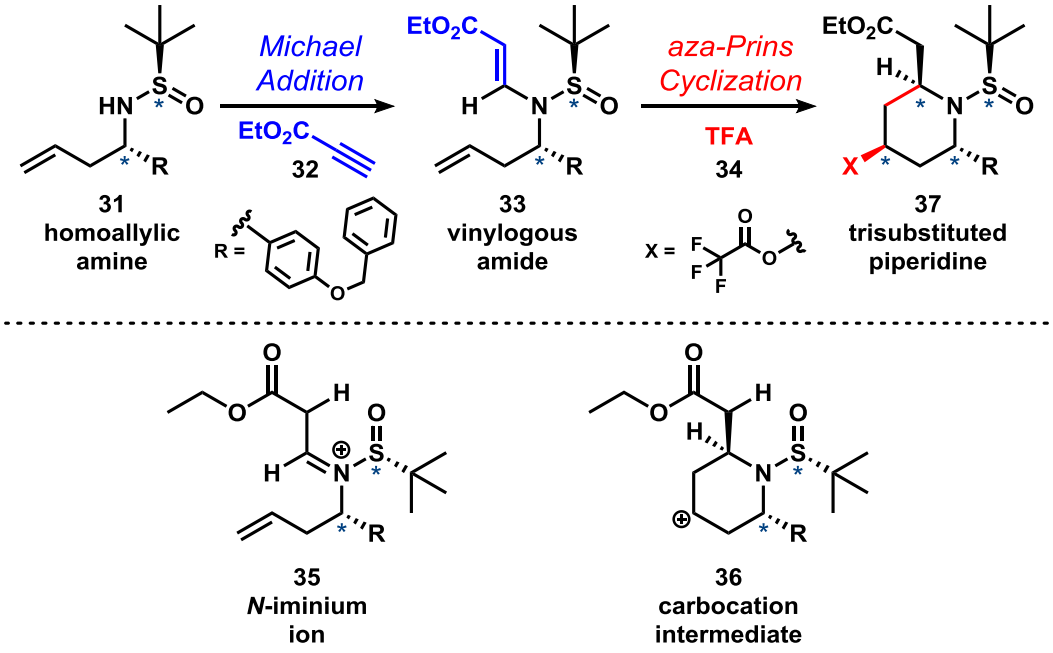

The Michael addition was first attempted without the removal of the sulfinyl group using basic sodium bis(trimethylsilyl)amide and equal equivalents of homoallylic amine and ethyl propriolate. The sodium bis(trimethylsilyl) amide was hypothesized to act as a strong base and deprotonate the homoallylic amine, making it a better Michael donor to react with the ethyl propiolate Michael acceptor to form the vinylogous amide. Unfortunately, after allowing the reaction to proceed for three hours, there was no consumption of starting material as monitored by HPLC.

It was then postulated that the sulfinyl group was too bulky and prevented the reaction from proceeding. The sulfinyl group was then deprotected to access the ammonium salt. The Michael reaction was then run in deuterated water (D_2O) with ethyl propiolate and homoallylic amine via published methods.[24] Monitoring the reaction progress via ^1H NMR found that no desired vinylogous amide formed via this method. It would be expected that

the product has new vinyl enamine protons located in the approximate 5 to 7 ppm region. Unfortunately, no new alkene protons were observed.

It was then theorized that the reaction was solvent dependent, and so a solvent screen was initialized. To that end, equal equivalents of ethyl propiolate and ammonium salt were reacted in basic conditions with Et_3N in a variety of solvents ranging in dielectric constants. These included water, toluene, tetrahydrofuran (THF), and DCM, but even after allowing the reactions to proceed for several days, ^{1}H NMR revealed no desired vinylogous amide formation. We therefore concluded that the *N*-sulfinyl amine was not sufficiently acidic to be deprotonated by triethylamine.

We now turned attention to more basic amines to deprotonate the homoallylic amine. Using equal equivalents of ethyl propiolate and ammonium salt, a trial was run with the organic base 4-dimethylaminopyridine (DMAP) and the aqueous base potassium carbonate. The reactions were allowed to stir overnight; however, after workup, the ^{1}H NMR revealed only recovered starting material with no desired vinylogous amide observed. At this point in time we decided to abandon these efforts at alkylating the *N*-sulfinyl amine.

4.7 Future Directions

In the immediate future, work will be invested in optimizing the reduction of succinimides as this is the most challenging aspect of this methodology. The reduction with DIBAL-H approximately afforded a 20% yield of *N*-acyl aminal as determined by ^{1}H NMR. We are interested in investigating the success of DIBAL-H when using excess equivalents as more may offer higher yields. Higher conversions here would benefit the identification of the *N*-acyl aminal as a spectral analysis would be viable. We plan to bring

the *para*-fluoro derivative through to the reduction step on larger scale to try alternative reduction conditions. Further, trialing a larger scale would afford the required amount of material for X-ray crystallography to confirm the chirality of the trisubstituted piperidine.

From our initial impressions of the cyclization reaction, this reaction should proceed smoothly in the future with *N*-acyl aminals. Once the reduction step is optimized, we envision that this work will allow for a straightforward methodology to access enantiopure trisubstituted piperidines. The remaining *N*-sulfinyl imines will then be submitted to this synthetic route to investigate this methodology's substrate versatility and create a library of structurally diverse trisubstituted piperidines for a manuscript.

5. References

1. Vitaku, E.; Smith, D. T.; Njardarson, J. T. Analysis of the Structural Diversity, Substitution Patterns, and Frequency of Nitrogen Heterocycles among U.S. FDA Approved Pharmaceuticals. *J. Med. Chem.* **2014**, *57* (24), 10257–10274.
2. Couladouros, E. A.; Strongilos, A. T.; Neokosmidis, E. Formal Synthesis of the Piperidine Alkaloid (±)-Prosophylline Using Polymer-Supported Dihydro-2H-Pyridin-3-One. *Tetrahedron Letters.* **2007**, *48* (46), 8227–8229.
3. Indukuri, K.; Unnava, R.; Deka, M. J.; Saikia, A. K. Stereoselective Synthesis of Amido and Phenyl Azabicyclic Derivatives via a Tandem Aza Prins-Ritter/Friedel–Crafts Type Reaction of Endocyclic N-Acyliminium Ions. *J. Org. Chem.* **2013**, *78* (21), 10629–10641.
4. Olier, C.; Kaafarani, M.; Gastaldi, S.; Bertrand, M. P. Synthesis of Tetrahydropyrans and Related Heterocycles via Prins Cyclization; Extension to Aza-Prins Cyclization. *Tetrahedron.* **2010**, *66* (2), 413–445.
5. Cuthbertson, J. D.; Taylor, R. J. K. A Telescoped Route to 2,6-Disubstituted 2,3,4,5-Tetrahydropyridines and 2,6-Syn-Disubstituted Piperidines: Total Synthesis of (−)-Grandisine G. *Angew. Chem. Int. Ed.* **2013**, *52* (5), 1490–1493.
6. Farina, V.; Reeves, J. T.; Senanayake, C. H.; Song, J. J. Asymmetric Synthesis of Active Pharmaceutical Ingredients. *Chem. Rev.* **2006**, *106* (7), 2734–2793.
7. DiMasi, J. A.; Grabowski, H. G.; Hansen, R. W. Innovation in the Pharmaceutical Industry: New Estimates of R&D Costs. *Journal of Health Economics.* **2016**, *47*, 20–33.
8. Vargesson, N. Thalidomide-Induced Teratogenesis: History and Mechanisms. *Birth Defect Res. C* **2015**, *105* (2), 140–156.
9. Alibés, R.; Bayón, P.; de March, P.; Figueredo, M.; Font, J.; García-García, E.; González-Gálvez, D. An Effective Enantioselective Approach to the Securinega Alkaloids: Total Synthesis of (−)-Norsecurinine. *Org. Lett.* **2005**, *7* (22), 5107–5109.
10. Saikia, A. K.; Indukuri, K.; Das, J. Stereoselective Synthesis of O-Tosyl Azabicyclic Derivatives via Aza Prins Reaction of Endocyclic N-Acyliminium Ions: Application to the Total Synthesis of (+/-)-Epi-Indolizidine 167B and 209D. *Org. Biomol. Chem.* **2014**, *12* (36), 7026–7035.
11. Reddy, P. Y.; Kondo, S.; Toru, T.; Ueno, Y. Lewis Acid and Hexamethyldisilazane-Promoted Efficient Synthesis of N-Alkyl- and N-Arylimide Derivatives. *J. Org. Chem.* **1997**, *62* (8), 2652–2654.
12. Robak, M. T.; Herbage, M. A.; Ellman, J. A. Synthesis and Applications of Tert-Butanesulfinamide. *Chem. Rev.* **2010**, *110* (6), 3600–3740.
13. Cogan, D. A.; Liu, G.; Ellman, J. Asymmetric Synthesis of Chiral Amines by Highly Diastereoselective 1,2-Additions of Organometallic Reagents to N-Tert-Butanesulfinyl Imines. *Tetrahedron.* **1999**, *55* (29), 8883–8904.
14. Chen, X.-Y.; Sun, L.-S.; Gao, X.; Sun, X.-W. Diastereoselective Allylation of N-Tert-Butanesulfinyl Imines: An Asymmetric Synthesis Experiment for the Undergraduate Organic Laboratory. *J. Chem. Educ.* **2015**, *92* (4), 714–718.

15. Sun, X.-W.; Xu, M.-H.; Lin, G.-Q. Room-Temperature Highly Diastereoselective Zn-Mediated Allylation of Chiral N-Tert-Butanesulfinyl Imines: Remarkable Reaction Condition Controlled Stereoselectivity Reversal. *Org. Lett.* **2006**, *8* (21), 4979–4982.
16. Foubelo, F.; Yus, M. Diastereoselective Indium-Promoted Allylation of Chiral N-Sulfinyl Imines. *Eur. J. Org. Chem.* **2014**, *2014* (3), 485–491.
17. Prakash G. K. Surya; Mandal Mihirbaran; Olah George A. Stereoselective Nucleophilic Trifluoromethylation of N- (Tert- Butylsulfinyl)Imines by Using Trimethyl(Trifluoromethyl)Silane. *Angewandte Chemie International Edition.* **2001**, *40* (3), 589–590.
18. Butters, M.; Davies, C. D.; Elliott, M. C.; Hill-Cousins, J.; Kariuki, B. M.; Ooi, L.; Wood, J. L.; Wordingham, S. V. Synthesis and Stereochemical Determination of Batzelladine C Methyl Ester. *Org. Biomol. Chem.* **2009**, *7* (23), 5001–5009.
19. Polniaszek, R. P.; Belmont, S. E.; Alvarez, R. Stereoselective Nucleophilic Additions to the Carbon-Nitrogen Double Bond. 3. Chiral Acyliminium Ions. *J. Org. Chem.* **1990**, *55* (1), 215–223.
20. Sadovoy, A.; Kovrov, A.; Golubeva, G.; Sviridova, L. Regioselective Synthesis of 1-Alkyl-5-(Indol-3-Yl- and -2-Yl)Pyrrolidin-2-Ones from Available Reagents. *Chemistry of Heterocyclic Compounds.* **2011**, *46* (10), 1215–1223.
21. Reddy, P. Y.; Kondo, S.; Toru, T.; Ueno, Y. Lewis Acid and Hexamethyldisilazane-Promoted Efficient Synthesis of N-Alkyl- and N-Arylimide Derivatives. *J. Org. Chem.* **1997**, *62* (8), 2652–2654.
22. Wu, P.; Nielsen, T. E. Scaffold Diversity from N-Acyliminium Ions. *Chem. Rev.* **2017**, *117* (12), 7811–7856.
23. Minch Michael J. Orientational Dependence of Vicinal Proton- proton NMR Coupling Constants: The Karplus Relationship. *Concepts in Magnetic Resonance.* **2005**, *6* (1), 41–56.
24. Randive, N. A.; Kumar, V.; Nair, V. A. A Facile Approach to Substituted Acrylates by Regioselective and Stereoselective Addition of Thiols and Amines to an Alkynyl Ester in Water. *Monatshefte für Chemie - Chemical Monthly.* **2010**, *141* (12), 1329–1332.

6. Supporting Information

(*R*,E)-*N*-(4-fluorobenzylidene)-2-methylpropane-2-sulfinamide (20a): To a 100 mL single neck round bottom flask was added *para*-fluorobenzaldehyde (1.073 mL, 10 mmol), triisopropyl borate (6.97 mL, 30.0 mmol), and (*R*)-2-methylpropane-2-sulfinamide (1.454 g, 12.00 mmol) to yield a light brown colored suspension that was aged at 70˚C. After twenty-three hours, HPLC and TLC revealed consumption of *para*-fluorobenzaldehyde. The light-yellow reaction solution was then allowed to cool to room temperature and was diluted with water (25 mL) and ethyl acetate (25 mL). The reaction mixture was then stirred vigorously for one hour. The reaction mixture was then extracted with ethyl acetate (two 25 mL portions). The combined organic layers were then washed with brine (25 mL), dried over magnesium sulfate, filtered, and concentrated via rotary evaporator to yield a yellow oil. The resultant oil was then placed under vacuum overnight to yield (*R*,E)-*N*-(4-fluorobenzylidene)-2-methylpropane-2-sulfinamide (2.2043 g, 97%) as yellow oil. IR (thin film) 1600 cm^{-1}; 1H NMR ($CDCl_3$, 400 MHz) δ: 8.55 (s, 1H), 7.86 (dd, J = 8.8, 5.4 Hz, 2H)* magnetically inequivalence, 7.16 (dd, J = 8.6, 8.6 Hz, 2H)* magnetically inequivalence, 1.26 (s, 9H); 13C NMR ($CDCl_3$, 100MHz) δ: 165.3 (s, J = 254.9 Hz), 161.4 (d), 131.5 (d, J = 9.3 Hz), 130.6 (s, J = 3.0 Hz), 116.2 (d, J = 22.1 Hz), 57.8 (s), 22.6 (q);

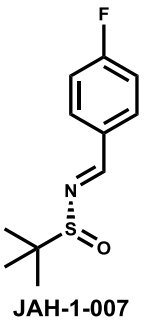

JAH-1-007

(*R*,E)-*N*-(3-fluoro-4-hydroxybenzylidene)-2-methylpropane-2-sulfinamide (20b): To a 50 mL single neck round bottom flask was added 3-fluoro-4-hydroxybenzaldehyde (2.000 g, 14.27 mmol), triisopropyl borate (11.60 mL, 50.0 mmol), and (*R*)-2-methylpropane-2-sulfinamide (2.162 g, 17.84 mmol) to give a light brown colored suspension that was aged at 70˚C. HPLC and TLC revealed consumption of 3-fluoro-4-hydroxybenzaldehyde after five hours. The solution was then allowed to cool to room temperature before diluting with water (25 mL) and ethyl acetate (25 mL). The resultant solution was stirred vigorously for one hour before extracting with ethyl acetate (two 25 mL portions). The combine organic phase was then dried over magnesium sulfate, filtered, and concentrated via rotary evaporator to afford (*R*,E)-N-(3-fluoro-4-hydroxybenzylidene)-2-methylpropane-2-sulfinamide (3.700 g, 107%) as white solid. mp 187-191˚C; IR (thin film) 3176, 1606 cm^{-1}; 1H NMR (DMSO-d_6, 400 MHz) δ: 8.41 (s, 1H), 7.72 (dd, J = 11.8, 1.9 Hz, 1H), 7.63 (dd, 8.4, 1.6 Hz, 1H), 7.08 (dd, J = 8.6, 8.6 Hz, 1H), 6.53 (s, 1H), 1.16 (s, 9H); 13C NMR (DMSO-d_6, 100MHz) δ: 161.7 (d, J = 3.0 Hz), 151.5 (s, J = 242.3 Hz), 149.9 (s, J = 12.0 Hz), 127.6 (d, J = 2.0 Hz), 126.3 (s, J = 6.1 Hz), 118.4 (d, J = 3.0 Hz), 116.8 (d, J = 18.8 Hz), 57.6 (s), 22.5 (q);

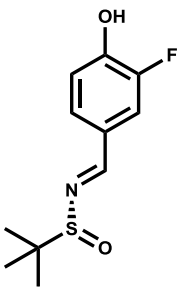

JAH-1-001

(*R*,E)-*N*-(4-hydroxy-3-methoxybenzylidene)-2-methylpropane-2-sulfinamide (20c):

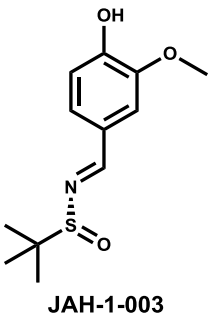

JAH-1-003

To a 50 mL single neck round bottom flask was added 4-hydroxy-3-methoxybenzaldehyde (2.000 g, 13.15 mmol), triisopropyl borate (10.68 mL, 46.0 mmol), and (*R*)-2-methylpropane-2-sulfinamide (16.43 mmol, 1.991 g) to give a light brown colored suspension that was aged at 70˚C. After nineteen hours, HPLC and TLC revealed consumption of the 4-hydroxy-3-methoxybenzaldehyde. The solution was then allowed to cool to room temperature and was diluted with water (25 mL) and ethyl acetate (25 mL). The reaction mixture was then stirred vigorously for one hour. The reaction solution was then extracted ethyl acetate (one 50 mL portion). The combined organic layers were then dried over magnesium sulfate, filtered, and concentrated via rotary evaporator to afford (*R*,E)-*N*-(4-hydroxy-3-methoxybenzylidene)-2-methylpropane-2-sulfinamide (3.700 g, 110%) as a light yellow oil. IR (thin film) 3216, 1591 cm^{-1}; 1H NMR ($CDCl_3$, 400 MHz) δ: 8.47 (s, 1H), 7.42 (d, J = 1.8 Hz, 1H), 7.35 (dd, 8.2, 1.8 Hz, 1H), 7.00 (d, J = 8.1 Hz, 1H), 6.17 (s, 1H), 3.97 (s, 3H), 1.26 (s, 9H); 13C NMR ($CDCl_3$, 100MHz) δ: 161.7 (d), 153.1 (s), 131.2 (d), 122.5 (s), 111.4 (d), 57.3 (s), 40.1 (q), 22.5 (q);

(*R*,E)-*N*-(4-(dimethyamino)benzylidene)-2-methylpropane-2-sulfinamide (20d): To a

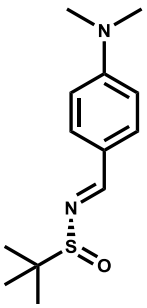

JAH-1-008

100 mL single neck round bottom flask was added 4-(dimethylamino)benzaldehyde (1.492 g, 10 mmol), triisopropyl borate (20.97 mL, 90 mmol), and (*R*)-2-methylpropane-2-sulfinamide (1.454 g, 12.00 mmol) to yield a light brown colored suspension that was aged at 70˚C. After 30 hours, HPLC and TLC revealed 4-(dimethylamino)benzaldehyde remained in the vessel. Another 0.1 equivalent (0.121g) of (R)-2-methylpropane-2-sulfinamide was added. After forty-eight hours, HPLC revealed 4% 4-(dimethylamino)benzaldehyde, 90% (*R*,E)-N-(4-(dimethykamino)benzylidene)-2-methylpropane-2-sulfinamide, and 6% unknown. The dark brown reaction mixture was allowed to cool to room temperature and was transferred to a 250-mL single neck round bottom flask. The solution was then diluted with water (50 mL) and ethyl acetate (50 mL) and allowed to stir for one hour. The reaction mixture was then extracted with ethyl acetate (three 25 mL portions). The combined organic layers were washed once with brine (25 mL), dried over magnesium sulfate, filtered, and concentrated via rotary evaporator. The brown oil was then placed on high vacuum overnight to yield (*R*,E)-*N*-(4-(dimethykamino)benzylidene)-2-methylpropane-2-sulfinamide (3.700g, 147%) as a brown solid. 65-68 mp ˚C; IR (thin film) 1606 cm-1; 1H NMR (CDCl3, 400 MHz) δ: 8.43 (s, 1H), 7.72 (d, J = 8.9 Hz, 2H), 6.70 (d, 8.9 Hz, 2H), 3.06 (s, 6H), 1.23 (s, 9H); 13C NMR (CDCl3, 100MHz) δ: 161.7 (d), 153.1 (s), 131.2 (d), 122.5 (s), 111.4 (d), 57.3 (s), 40.1 (q), 22.5 (q);

(*R*,E)-2-methyl-*N*-(pyridin-3-ylmethylene)propane-2-sulfinamide (20e): To a 100 mL single neck round bottom flask was added nicotinaldehyde (0.939 mL, 10 mmol), triisopropyl borate (6.97 mL, 30.0 mmol) , and (*R*)-2-methylpropane-2-sulfinamide (1.454 g, 12.00 mmol) to give a light brown colored suspension that was aged at 70˚C. After seven and a half hours, HPLC and TLC revealed consumption of nicotinaldehyde. The solution was then allowed to cool to room temperature and was diluted with water (25 mL) and ethyl acetate (25 mL). The light-yellow reaction mixture was then stirred vigorously for one hour. The reaction mixture was then extracted with ethyl acetate (two 25 mL portions). The combined organic layers were then washed with brine (25 mL), dried over magnesium sulfate, filtered, and concentrated via rotary evaporator to yield (*R*,E)-2-methyl-*N*-(pyridin-3-ylmethylene)propane-2-sulfinamide (2.000 g, 95%) as yellow oil. IR (thin film) 1608 cm^{-1}; 1H NMR (CDCl3, 400 MHz) δ: 9.03 (d, J = 1.4 Hz, 1H), 8.74 (dd, J = 4.7, 1.4 Hz, 1H), 8.64 (s, 1H), 8.17 (ddd, J = 7.9, 1.7, 1.7 Hz, 1H), 7.42 (dd, J = 4.7, 1.4 Hz, 1H), 1.28 (q, 9H); 13C NMR ($CDCl_3$, 100MHz) δ: 160.4 (d), 152.9 (d), 151.0 (d), 135.7 (d), 129.7 (s), 123.9 (d), 58.1 (s), 22.6 (q);

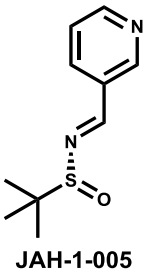

JAH-1-005

(*R*,E)-*N*-(3,4-dimethyloxybenzylidene)-2-methylpropane-2-sulfinamide (20f): To a 100 mL single neck round bottom flask was added 3,4-dimethoxybenzaldehyde (1.662 g, 10 mmol), triisopropyl borate (20.97 mL, 90 mmol), and (*R*)-2-methylpropane-2-sulfinamide (1.454 g, 12.00 mmol) to yield a light brown colored suspension that was aged at 70˚C. After twenty-six hours, HPLC and TLC revealed consumption of 3,4-dimethoxybenzaldehyde. The deep orange solution was then allowed to cool to room temperature. The reaction solution was then transferred to a 250-mL single neck round bottom flask and diluted with water (75 mL) and ethyl acetate (25 mL). The reaction mixture was stirred vigorously for one hour and extracted with ethyl acetate (two 25 mL portions). The combined organic layers were then washed with brine (25 mL), dried over magnesium sulfate, filtered, and concentrated by rotary evaporation to yield yellow oil. The resultant oil was then placed under vacuum overnight to yield (*R*,E)-*N*-(3,4-dimethyloxybenzylidene)-2-methylpropane-2-sulfinamide (2.9097 g, 108%) as yellow solid. mp 53-60 ˚C; IR (thin film) 1596 cm^{-1}; 1H NMR ($CDCl_3$, 400 MHz) δ: 8.49 (s, 1H), 7.44 (d, J = 8.3 Hz, 1H), 7.73 (dd, 8.3, 1.3 Hz, 1H), 6.93 (d, J = 1.7 Hz, 1H), 3.94 (s, 3H), 3.94 (s, 3H), 1.26 (s, 9H); 13C NMR ($CDCl_3$, 100MHz) δ: 162.0 (d), 152.9 (s), 149.5 (s), 127.5 (s), 125.0 (d), 110.7 (d), 109.9 (d), 57.6 (s), 56.0 (q), 55.9 (q), 22.6 (q);

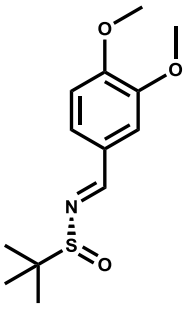

JAH-1-006

(*R*)-*N*-((*S*)-1-(4-fluorophenyl)but-3-en-1-yl)-2-methylpropane (22a): To a 250 mL single neck round bottom flask was added (*R*,E)-N-(4-fluorobenzylidene)-2-methylpropane-2-sulfinamide (4.945 g, 21.76 mmol), DMF (108.7 mL, 21.76 mmol), and allyl bromide (3.76 mL, 43.51 mmol) to yield a light yellow solution. Indium (3.247 g, 28.28 mmol) was then added in one portion generating a yellow-grey solution. The vessel was then heated to 70˚C. After 23 hours, 1H NMR revealed 6% of imine starting material remaining and so the reaction was allowed to age longer. After 44, 1H NMR revealed complete consumption of the starting material. The reaction was then allowed to cool, and water (100 mL) was added. The reaction was allowed to stir overnight. After 68 hours, the reaction was transferred to a 500 mL single neck flask. Ethyl acetate (100 mL) was then added and the reaction was allowed to stir for 6 hours. The reaction cocktail was then extracted twice with ethyl acetate (100 mL). The organic layer was then dried with MgSO4, gravity filtered, and concentrated under house. Approximately, 75 mL of DMF remained in the flask after several hours. Ethyl acetate (100 mL) was then added and the solution was washed five times with distilled water (100 mL) to remove excess water. The last wash resulted in a very cloudy emulsion that was resolved by adding brine (100 mL). The organic phase was then dried with $MgSO_4$ and gravity filtered producing a yellow solution. (*R*)-N-((*S*)-1-(4-fluorophenyl)but-3-en-1-yl)-2-methylpropane-2-sulfinamide (4.777g, 82%) was collected as yellow solid. mp 92-96˚C; IR (thin film) 3203, 3073 cm^{-1}; 1H NMR ($CDCl_3$, 400 MHz) δ: 7.29 (dd, 8.6, 5.4 Hz, 2H), 7.02 (dd, 8.8, 8.8 Hz, 2 H), 5.71 (dddd, 17.9, 9.4, 8.4, 5.9 Hz, 1H), 5.17 (d, 15.5 Hz, 1H), 5.17 (d, 11.9 Hz, 1H), 4.46 (ddd, 7.8, 5.5, 1.8 Hz, 1H), 3.69 (br s, 1H), 2.52-2.60 (m, 1H), 2.40-2.50 (m, 1H), 1.19 (s, 9H); 13C NMR ($CDCl_3$, 100MHz) δ: 162.2 (s, J = 245.2 Hz), 137.3 (s, J = 3.3 Hz), 133.9 (d), 129.1 (d, J = 8.5 Hz), 119.4 (t), 115.6 (d, J = 21.2 Hz), 56.3 (d), 55.6 (s), 43.4 (t), 22.6 (q);

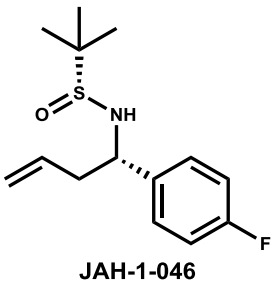

JAH-1-046

(*S*)-1-(4benzyloxy)phenyl)but-3-en-1-aminium (23a): To a 50 mL single round bottom flask,(*S*)-*N*-(1-(4-(benzyloxy)phenyl)but-3-en-1-yl)-2-methylpropane -2-sulfinamide (0.996 g, 2.786 mmol) was dissolved in diethyl ether (9.29 mL, 2.79 mmol) at room temperature. After 30 minutes particulates still remained in solution and diethyl ether was added (10 mL). 4 M HCl in dioxane (2.089 mL, 8.359 mmol) was then added in one portion, and the reaction immediately turned yellow upon addition. The reaction was then allowed to stir for 5 minutes at room temperature while a thick white precipitate formed. HPLC and TLC revealed the consumption of starting material. (Starting material had retention time of 7.744 and product had retention time of 5.241.) The (*S*)-1-(4benzyloxy)phenyl)but-3-en-1-aminium (0.6821 g, 84%) was collected via vacuum filtration as a white precipitate using chilled diethyl ether. mp 179-181˚C; IR (thin film) 3419, 3035 cm^{-1}; 1H NMR ($CDCl_3$, 400 MHz) δ: 8.62 (br s, 3H), 7.27-7.41 (m, 7H), 6.94 (d, 8.6 Hz, 2H), 5.55 (dddd, 17.0, 9.8, 7.0, 7.0 Hz), 5.08 (br d, 16.6 Hz, 1H), 5.03 (br d, 10.2 Hz, 1H), 4.99 (s, 2H), 4.16 (br s, 1H), 2.77-2.88 (m, 1H), 2.63-2.75 (m, 1H); 13C NMR ($CDCl_3$, 100MHz) δ: 159.2 (s), 136.6 (s), 131.8 (d), 129.0 (d), 128.6 (d), 128.1 (d), 128.0 (t), 127.6 (d), 120.0 (t), 115.2 (d), 70.0 (t), 55.4 (d), 38.7 (t)

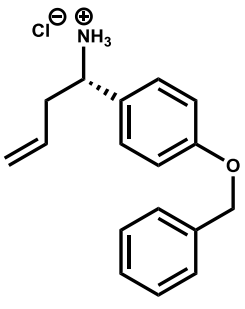

JAH-1-022

(*S*)-1-(4-fluorophenyl)but-3-en-1-amine (24a): (*S*)-chloro(1-(4-fluorophenyl)but-3-en-1-yl)-l5-azane (293 mg, 1.45 mmol) was dissolved in DCM (15 mL, 0.23 mol) at room temperature. Sodium hydroxide pellet (116 mg, 2.91 mmol) was then added followed by water (1.5 mL, 83 mmol). The reaction was allowed to stir for 19 hours before extracting twice with DCM (two 15 mL portions). The resultant organic layers were combined, dried with $MgSO_4$, and concentrated over house air to yield (*S*)-1-(4-fluorophenyl)but-3-en-1-amino (200.5 mg, 84%) as yellow oil. IR (thin film) 3078, 1595 cm^{-1}; 1H NMR ($CDCl_3$, 400 MHz) δ: 7.29 (dd, 8.3, 5.8 Hz, 2H), 6.99 (dd, 8.6, 8.6 Hz, 2H), 5.71 (dddd, 16.8, 10.2, 8.0, 6.5 Hz, 1H), 5.09 (d, 14.4 Hz, 1H), 5.09 (d, 8.3 Hz, 1H), 3.97 (dd, 7.6, 6.0 Hz, 1H), 2.36-2.45 (m, 1H), 2.25-2.36 (m, 1H), 1.72 (s, 2H); 13C NMR ($CDCl_3$, 100MHz) δ: 161.8 (s, J = 243.1 Hz), 141.4 (s, J = 3.0 Hz), 135.2 (d), 127.8 (d, J = 8.0 Hz), 117.8 (t), 115.1 (d, J = 21.0 Hz), 54.7 (d), 44.3 (t), 43.4 (t);

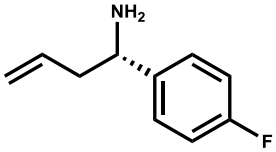

JAH-1-051

(*S*)-1-(1-(4fluorophenyl)but-3-en-1-yl)pyrrolidine-2,5-dione (27a): To a 50 mL round bottom vial was added (*S*)-1-(4-fluorophenyl)but-3-en-1-amine (110.8 mg, 670.7 μmol) and succinic anhydride (67.11 mg, 670.7 μmol) in toluene (8.38 mL, 670.7 μmol). Zinc chloride (91.40 mg, 670.7 μmol) was then added in one portion. The reaction vessel was then heated to 85˚C and aged for ten minutes. Bis(trimethylsilyl)amine (HMDS) (212 μL, 1.006 mmol) was then added in one portion. After 27 hours, TLC revealed the consumption of starting material. The reaction was then allowed to cool to room temperature. 0.5 N HCl (25 mL) was then added in one portion and the reaction mixture was allowed to stir for five minutes. The resultant solution was then extracted twice with ethyl acetate (two 20 mL portions). The combined organic layers were then washed once with saturated sodium bicarbonate (20 mL) and once with brine (20 mL). The organic layer was then separated, dried over $MgSO_4$, gravity filtered, and concentrated to yield (*S*)-1-(1-(4fluorophenyl)but-3-en-1-yl)pyrrolidine-2,5-dione (146.1 mg, 88%) as a yellow oil. IR (thin film) 3065, 1704 cm^{-1}; 1H NMR ($CDCl_3$, 400 MHz) δ: 7.48 (dd, 8.6, 5.4 Hz, 2H), 7.00 (dd, 8.0, 8.0 Hz, 2H), 5.69 (dddd, 17.1, 10.2, 8.5, 5.5 Hz, 1H), 5.27 (dd, 10.5, 6.1 Hz, 1H), 5.12 (dddd, 17.0, 1.6, 1.6, 1.6 Hz, 1H), 5.06 (br d, 10.0 Hz, 1H), 3.28 (ddddd, 14.2, 10.2, 8.4, 0.7, 0.7 Hz, 1H), 2.84 (ddddd, 14.4, 6.0, 6.0, 1.5, 1.5 Hz, 1H), 2.63 (s, 4H); 13C NMR ($CDCl_3$, 100MHz) δ: 177.1 (s), 162.4 (s), 134.2 (s), 134.1 (d), 130.1 (d, J = 8.2 Hz), 118.3 (t), 115.3 (d, J = 21.5 Hz), 54.1 (d), 34.4 (t), 27.9 (t);

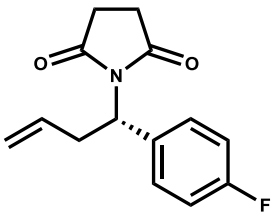

JAH-1-053

***N*-(5-(4-fluorophenyl)-3-oxooctahydroindolizin-7-yl)acetamide-2,2,2-d$_3$ (29):** To a

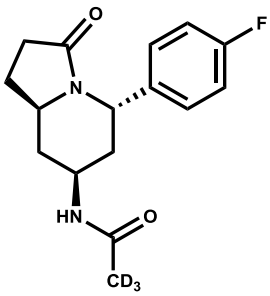

JAH-1-067

flame dried 25 mL round bottom was added (*S*)-1-(1-(4-fluorophenyl)but-3-en-1-yl)pyrrolidine-2,5-dione (100 mg, 404 μmol)and DCM (4.04 mL, 404 μmol) under a nitrogen atmosphere to generate a light yellow solution. The flask was then placed in a dry ice/acetone bath for ten minutes. Diisobutylaluminum hydride (404 μL, 404 μmol) (1M in DCM) was then added slowly over fifteen minutes (one drop every 10 sec with a 12 gauge needle). TLC in 9:1 DCM:methanol revealed imide spot at 0.80 and new spot at 0.50 after fifteen minutes. After 15 minutes, TLC revealed reaction progress had stalled. The reaction was allowed to stir for an hour before it was removed from the dry ice/acetone bath. Immediately, the reaction was quenched with ammonium chloride (5 mL) added dropwise by pipette. The ammonium chloride froze and the reaction was allowed to stir until it warmed to room temperature. The reaction was then extracted twice with DCM (10 mL). The combined organic layers were washed with brine (10 mL) and separated. The organic layers were then dried over $MgSO_4$ and gravity filtered. The material was concentrated over house air to afford 112 mg of yellow oil. 1H NMR revealed about a 20% conversion of the imide to potential *N*-acyl aminal. In an NMR tube was added 1-((*S*)-1-(4-fluorophenyl)but-3-en-1-yl)-5-hydroxypyrrolidin-2-one (26 mg, 0.10 mmol) (crude reaction material from the reduction) in acetonitrile-d3 (1.0 mL, 0.10 mmol) to generate a yellow solution. Then BF_3•OEt_2 (26 μL, 0.21 mmol) was then added in one portion. The reaction was vortexed for five minutes. After four hours, the reaction stalled and another equivalent of BF_3•OEt_2 (26 μL, 0.21 mmol) was added. The reaction was allowed to stir for 72 hours with no more progession observed. The NMR tube contents were transferred to a 125 mL sep funnel and 2 mL of saturated sodium bicarbonate was added slowly. The mixture was shaken for one minute before extracting twice with DCM (10 mL). The combined organic layers were then washed once with brine (10 mL), dried over $MgSO_4$, and concentrated to 41 mg of yellow oil. The yellow oil was loaded onto a 4g silica gel column with DCM. The column was eluted with 5% methanol in DCM (25 mL) into fifteen fractions (1.5 mL). The *N*-(5-(4-fluorophenyl)-3-oxooctahydroindolizin-7-yl)acetamide-2,2,2-d$_3$ was collected (10.0 mg, 10%) as a white solid. IR (thin film) 3287, 1657 cm^{-1}; 1H NMR ($CDCl_3$, 400 MHz) δ: 7.28 (dd, 8.4, 5.4 Hz, 2H), 7.03 (dd, 8.7, 8.7 Hz, 2H), 5.52 (d, 5.4 Hz, 1H), 5.42 (d, 7.1 Hz, 1H), 4.08 (ddddd, 11.9, 11.9, 7.5, 3.7, 3.7 Hz, 1H), 3.64 (dddd, 11.4, 7.9, 6.0, 3.6 Hz, 1H), 2.63 (dddd, 13.3, 3.5, 1.7, 1.7 Hz, 1H), 2.48-2.55 (m, 2H), 2.27 (dddd, 13.8, 9.1, 7.9, 6.1 Hz, 1H), 2.15 (dddd, 12.0, 3.7, 3.7, 1.7 Hz, 1H), 1.66 (dddd, 13.2, 9.0, 9.0, 6.0 Hz, 1H), 1.60 (ddd, 13.2, 12.6, 5.9 Hz, 1H), 1.13 (ddd, 11.8, 11.8, 11.8 Hz, 1H); 13C NMR ($CDCl_3$, 100MHz) δ: 174.1 (s), 163.2 (s), 162.0 (s, J = 246.0 Hz), 133.9 (s, J = 3.3 Hz), 128.3 (d, J = 8.1 Hz), 115.7 (d, J = 21.5 Hz), 52.6 (d), 49.1 (d), 43.1 (d), 40.0 (t), 33.6 (t), 30.0 (t), 30.0 (s), 24.5 (t);